4-2018

Numerical Analysis of a Compact Helical Counterflow Heat Exchanger

Manikandan Chidambaram

NUMERICAL ANALYSIS OF A COMPACT HELICAL COUNTERFLOW HEAT EXCHANGER

By
Manikandan Chidambaram

A thesis
Submitted to
Florida Institute of Technology
In partial fulfillment of the requirements
For the degree of

Master of Science
In
Aerospace Engineering

Melbourne, Florida
April 2018

We, the undersigned committee, hereby recommend that the attached document be accepted as fulfilling in part the requirements for the degree of Master of Science in Aerospace Engineering

NUMERICAL ANALYSIS OF A COMPACT HELICAL COUNTERFLOW HEAT EXCHANGER

by
Manikandan Chidambaram
Master of Science
Aerospace Engineering
Florida Institute of Technology

_____

Daniel Kirk, Ph.D., Major Advisor
Associate Dean for Research,
Aerospace and Mechanical Engineering

_____

Hamidreza Najafi, Ph.D.,
Assistant Professor,
Aerospace and Mechanical Engineering

_____

Troy Nguyen, Ph.D.,
Associate Professor,
Civil Engineering – Construction Mgmt

_____

Hamid Hefazi, Ph.D.,
Professor and Department Head,
Aerospace and Mechanical Engineering

NUMERICAL ANALYSIS OF A COMPACT HELICAL COUNTERFLOW HEAT EXCHANGER

Manikandan Chidambaram

Dr. Daniel R. Kirk, Major Advisor

Abstract

The performance of compact counter flow heat exchangers with helically shaped passages is examined using a 1-D analytical model and compared with a high-fidelity 3-D numerical simulation. The 1-D model is capable of assessing the general trends associated with the heat transfer performance and fluid pressure losses, whereas the high fidelity 3-D numerical model is needed to provide more accuracy. For water flow rates of 0.01 kg/s -1 kg/s, the models are used to predict the overall heat transfer coefficient ratio for a straight and counter helix heat exchanger. The maximum difference between the 3-D numerical and 1-D analytical model for heat transfer performance is 2.6%, with larger disagreement associated with the fluid pressure drop of up to 37.5%. The primary reason for the deviation of the numerical results is attributable to secondary flow effects, which are neglected in the 1-D analytical model. Heat exchanger performance was studied by varying the geometric parameters such as the length and the number of turns per length of the heat exchanger, number of fins within the flow passages, inner and outer channel heights, and fin and wall thickness. Heat transfer rate and pressure drop on straight and helical fins heat exchangers were compared by keeping the length of the fin and the hydraulic diameter of the channel constant. Ultimately, the heat transfer rate for a helical design is found to increase by 56% as compared with a conventional counterflow heat exchanger of the same length and outer diameter. Furthermore, by using a helical flow path, the volume of the device can be reducing by 33%.

Table of Contents

List of Figures

List of Tables

List of Symbols

A	=	Area	[m^2]
C	=	Specific heat	[J/kg-K]
D	=	Diameter	[m]
De	=	Dean number	
$\boldsymbol{f}$	=	frictional factor	
h	=	Convective heat transfer coefficient or Enthalpy of fluid	[$W/m^{2-}K$] or [J/kg]
K	=	Thermal conductivity	[W/m-K]
L	=	Heat exchanger length	[m]
$\dot{\boldsymbol{m}}$	=	Mass flow rate of fluid	[kg/s]
n	=	Number of fins	
N	=	Number of turns	
Nu	=	Nusselt number	
P	=	Wetted perimeter	[m]
p	=	Pressure	[kPa]
Pr	=	Prandtl number	
Q	=	Energy transfer rate	[J/s]
Re	=	Reynolds number	
t	=	Thickness	[m]
T	=	Temperature	[K]
U	=	Overall heat transfer coefficient	[$W/m^{2-}K$]

Greek Symbols

Δ	=	Parameter difference	
η	=	Efficiency	
μ	=	Dynamic Viscosity	[Pa-s]
ρ	=	Density	[kg/m3]
ψ	=	Helical Angle	[deg]
$\boldsymbol{\theta}$	=	Lean angle	[deg]

Subscripts

ach	=	Achievable
crs	=	Cross-sectional area
c	=	Cold fluid
cric	=	Critical
cv	=	Curved pipe
f	=	Fins
h	=	Hot fluid or hydraulic
hlx	=	Helix
i or 1	=	Inlet or inner
lm	=	Log mean
o or 2	=	Outlet or outer
ovr	=	Overall
ratio	=	Ratio
req	=	Required
s	=	Straight or innermost

Acknowledgments

It would not have been possible to write this thesis without the help and support of many individuals who have contributed to the development of this thesis.

I would like to thank my advisor, Dr Daniel Robert Kirk for his support and advice in many aspects during my stay in FIT. Without his guidance and encouragement this study would hardly have been completed. I am also thankful to my panel members Dr Najafi and Dr Troy, who took time out of their busy schedule to help me in this thesis and to make it better.

My beloved and supportive family and lovable girlfriend who is always by my side when times I need them for most and supported me a lot in making this study. I am also grateful to my friends Aravind, Adwaith, Vignesh and Hari who have supported and helped me a lot throughout my master's degree.

1. Introduction

1.1. Background

Heat exchanger is a device used to transfer the thermal energy from one fluid to another fluid separated by suitable heat transfer surfaces. Heat exchangers are widely used in several industrial applications. They are used in aerospace and automobile applications, power plant industry, manufacturing industry, transportation power systems, chemical and medical field, air-conditioning, petroleum etc. They can be classified according to heat transfer process, construction, degrees of surface compactness, flow arrangements, pass arrangements, phase of process fluids and heat transfer mechanisms. The classification of the heat exchangers is explained briefly in chapter 2. Selecting the right heat exchanger for a particular problem, is a challenging task since several variables need to be considered. The most limiting factors in the construction of a heat exchanger are pressure drop, thermal performance, cost, range of fluid flow rate, maintenance and repair, material selections etc.

Heat transfer can be improved by increasing the surface area by means of fins, or it can be increased by choosing high thermal conductivity working fluid or changing the orientation of the channel and altering the geometry **[1]**. In this thesis, the first and third possible ways are chosen, i.e., by introducing helical fins to increase the heat transfer surface area and the orientation of the channel is changed by means of helical fins. Though these heat exchanger designs are compact (mass and volume) and increase the heat transfer rate, the construction of these designs (helical fin heat exchanger) are complicated with conventional manufacturing methods.

Compact heat exchangers are becoming more popular in modern days because of their high heat transfer rate within a smaller volume and weigh less when compared to conventional heat exchanger models. The evolution of the new manufacturing technologies such as 3D printing technology available in present days, has made the production of compact heat exchanger designs possible **[2]**. The potential of additive manufacturing technology is driven by the manufacturability of the complex designs with reduced cost when compared to traditional manufacturing methods. It also offers the functional designs without manufacturing limits and skip investment on manufacturing tools.

There are different types of 3D printing technologies are available based on the material selection. Fused deposition modeling (FDM), SLS Technology or laser sintering methods are used to print complex 3D designs with plastic and alumide. Stereolithography (SLA), Digital Light Processing (DLP), Continuous Liquid Interface Production (CLIP), Multijet printers are using resin or wax to print the models. Metals such as titanium, aluminum, stainless steel can be printed by DLP, Direct Metal Laser Sintering (DMLS) and Electron Beam Melting (EBM) **[3]**. The schematic view of the Direct Metal Laser sintering is shown below in Figure 1.

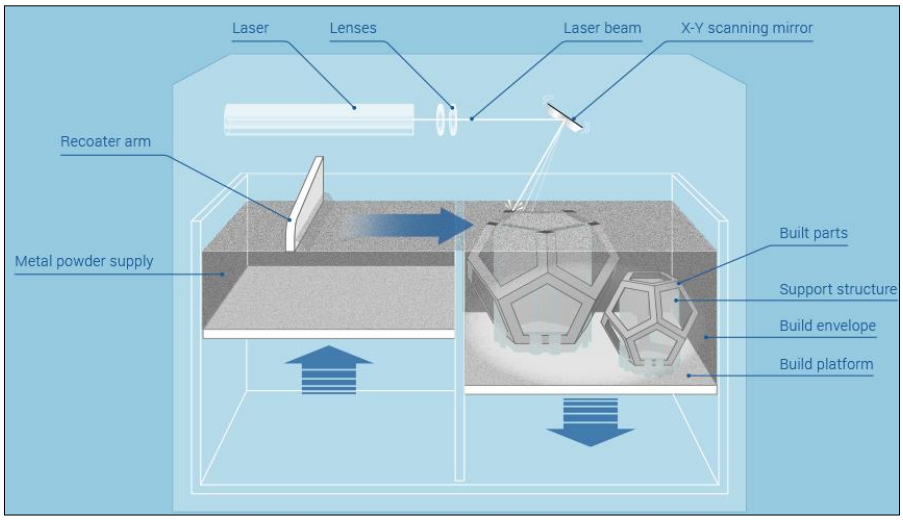

Figure 1-1 : SLM & EBM – Metal printing [3]

1.2. Motivation

Additive manufacturing has proven that it's capable of great things. For an example, NASA 3D printed a rocket part to reduce the future SLS engine costs **[4]**. It also stated that the 3D printing part eliminated more than 100 welds which reducing costs by nearly 35% and production time by more than 80%. In addition, they planned to build combustion chamber, nozzle, ducts, valves etc., using a variety of advanced manufacturing processes, which will eliminate more than 700 welds and more than 700 parts, while reducing engine cost.

The benefits of being able to build hollow structures with additive manufacturing may allow higher design complexity that may increases performance, as well as broaden the application range due to higher strength-to-weight ratios. These complex designs can be made with a favorable surface area, leading to the manufacturing of smart, efficient heat exchangers **[2]**. Experimentation is a major step involved in development of a modern designs such as the helical passage heat exchanger designs, but the facilities required for carrying out experimental analysis on all possible designs would be expensive. However, the development of software's such as computational fluid dynamics tool (CFD) with well validated models, suitable for variety of applications, can provide convenient and economic assistance in testing of innovative and newly designed models.

Experimental analysis on 3D printed helical heat exchangers are complicated due to its size constraints. Moreover, experimental work mainly focused on measuring the pressure and temperature at outlet and inlet of the heat exchanger whereas 3D numerical simulation can clearly figure out the flow phenomena inside the helical passage as well as can calculate the thermal performance of the heat exchanger.

1.3. Objectives

The main objective of this thesis are to:

- Assess the performance of a new compact counter flow heat exchanger design over a range of mass flow conditions and targeted heat exchange using 1-D analytical model.
- Assess a variety of geometric configurations for important performance metrics including heat exchanger, pressure loss, volume, mass, manufacturability, etc.
- Create 3-D virtual computer model of optimized heat exchanger designs.
- Determine heat exchanger performance such as outlet temperatures and fluid pressure drop using 3D numerical simulation by numerically simulate the flow through helical passage.

1.4. Approach

The first step is the creation of three-dimensional geometrical model of the current problem using CATIA software. To obtain conformal mesh between solid and fluid, the fluid volume is extracted from the solid volume using built in drawing module of the CFD software (ANSYS Design Modular) then converted to a single part. The grids for the computational domain is generated using ANSYS Fluent meshing tool. To capture the boundary layer effects (near wall effects on the fluid flow), the boundary layer thickness is calculated and included in meshing. The governing equations for steady turbulent flow and heat transfer on optimized helical heat exchangers are solved using the commercial CFD code ANSYS Fluent.

The secondary flow is visualized by illustrating the streamlines in cross-sections. Pressure drop, heat exchange through the heat transfer surface are illustrated in different planes along the heat exchanger length. The outlet temperature of hot and cold fluid is obtained using the surface integral.

1.5. Thesis Overview

Chapter 2 detailing about the classification of the heat exchangers and literature review of the conventional and modern compact heat exchangers

Chapter 3 discuss the overview of the counter flow heat exchanger and one dimensional analytical model to obtain the thermal performance and pressure drop across the heat exchanger. It also details the important results obtained from 1D analytical model for straight annular heat exchanger, helical fin heat exchanger and optimized helical fin heat exchangers.

Chapter 4 develops three-dimensional virtual computer heat exchanger model based on design proposed on analytical model and discuss the governing equations, assumptions and meshing of 3D heat exchanger design. This section also discusses the suitable turbulence and heat exchanger model to simulate the thermal and flow analysis.

Chapter 5 details the numerical results of the straight and optimized helical fin heat exchangers (pressure drop, and compactness prioritized, heat transfer and pressure drop prioritized,

compactness and heat transfer prioritized). It also includes the comparison of heat exchanger performance between the three-dimensional numerical analysis with one dimensional analytical model.

Chapter 6 conclude this thesis and summarizes the results of numerical analysis of optimized helical heat exchanger design and future work.

2. Literature Review

Due to the compact design and higher heat transfer rate, helical coil heat exchangers are extensively used in industrial applications. There have been many numerical and experimental studies carried out on helical coil heat exchanger. In literature, it has been widely reported that the helical coil heat exchangers are higher as compared to those in straight tubes **[5]**. The performance of helically coiled heat exchanger was investigated for heat removal system used in nuclear energy by Jayakumar. CFD simulation on helical coil heat exchanger has been carried out by varying geometry such as coil pitch, pipe diameter and pitch circle diameter have been studied and their influence on heat exchanger performance has been brought out. He also reported that unlike the flow through a straight pipe, the prediction of heat transfer coefficient is inaccurate with constant thermal properties of heat transport medium.

Heat transfer can be enhanced by increasing the heat transfer surface by incorporate extended surface such as fins. The heat transfer behaviors in developed and developing regions on four basic fins of plate fin heat exchanger was numerically analyzed by Yinhai Zhu and Yanzhong Li **[6]**. Three dimensional geometries such as plain fin, strip offset fin and wavy fin were investigated for the Reynolds number range of 132.3 to 1323. Data reduction method was used to calculate the local Nusselt number and pressure drop. Heat transfer characteristics were obtained using j and f factors.

Flow characteristics inside the helical pipe was analyzed by Lingadi Tang et al **[7]**. In this study, the numerical simulation was carried out to find velocity distribution, pressure field and secondary flow variation by varying coil parameters. It also stated that secondary flow is the major factor in pressure loss, however, increase in curvature radius and coil pitch can reduces

friction factor. The numerical method was validated by experimental analysis and found that the deviation between the numerical and experimental analysis was 2.9%.

The helical coil heat exchanger with different geometry such as coil pitch, pipe diameter and pitch circle diameter have been studied by J.S. Jayakumar **[5]**. It's been reported that the prediction of heat transfer coefficient is inaccurate with constant thermal and transport properties of heat transport medium. Higher heat transfer rate and less pressure drop for constant inlet velocity achieved by the influence of secondary flow with increasing pipe diameter. All his cases were considered, constant wall temperature and constant wall heat flux boundary conditions and observed that helical pipe has higher heat transfer rate than straight pipes due to the curvature of the pipe which in turn causes the secondary flow generation in helical pipes.

The characteristic of flow inside the helical coil, pressure drop, and heat transfer have been studied by many investigators. The performance of triangular finned tube heat exchanger was performed experimentally and numerically investigated by Vinous M. Hameed et al. Experimental work carried out by designing and manufacturing of triangular fins using copper material and the results showed that the enhancement of heat dissipation for triangular finned tube is 3 to 4 times than smooth tube. Numerical simulation was carried out using COMSOL CFD package model and reported that the numerical results showed good agreement with experimental work.

2.1. Classification of Heat Exchangers

Heat exchangers are thermal devices used for transferring thermal energy between fluidic materials in same or different phases. It is commonly used for exchange between a solid phased material and a fluid. A heat exchanger consists of input and output nozzles, a fluid circuit for the movement of the working fluid and a core containing the heat exchanger element. Heat is transferred between the fluids through the direct contact of the heat transfer surface present within the heat exchanger.

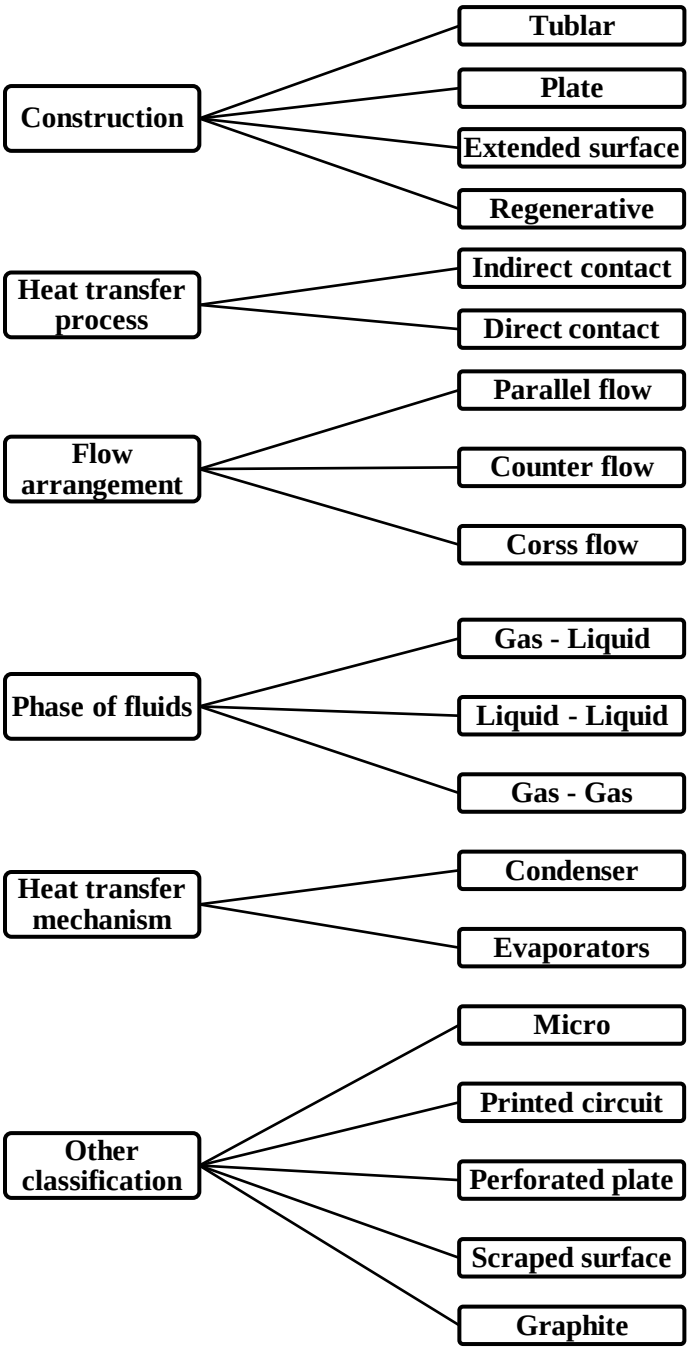

Figure 2-1 : Classification of heat exchangers

2.1.1. Classifications by Construction:

Tubular:

Tubular heat exchangers are the most commonly used type of heat exchanger for industrial purposes. It consists of concentric tubes having counter flow. The tubular heat exchangers are sub classified into several types, but the most frequently used are double pipe and shell and tube. The double pipe consists of two concentric pipes in the form of a U-bend design. The shell and tube consist of a shell within which several tubes which are enclosed in a rounded molded shell are placed for higher thermal exchange efficiency. The tubular heat exchangers are used for applications with high pressure specifications from 600 to 965 bars, this gives them an advantage over wide ranges of pressure **[8]**. In addition to this, tubular heat exchangers are cheap and as discussed useful for wide range of pressures and temperatures.

Plate:

Plate heat exchangers are less widely used in comparison to tubular heat exchangers. The working pressure and temperature of plate heat exchangers are less than 10 atm and 800°c, hence they are used in applications where the working fluid is a low or medium pressure liquid **[8]**. In processes which require heat transfer among production of sludge and slurry, spiral PHE are used as they require minimal maintenance whereas plate fin heat exchangers are used for gas to gas applications.

Extended surface:

Extended surface heat exchangers are most commonly found in automobile radiators, computer CPU heat sinks and in heat transfer applications within powerplants. These heat exchangers are used when the working fluid has low heat transfer coefficient, where large heat transfer surface area is required to increase the heat transfer rate. Extended surfaces which consists of fins of varied geometry are placed along the surface of the primary heat transfer element. These extended surfaces have higher rate of heat transfer due to better conduction to and from the fin surface because of reduction in temperature potential between fin and fluid.

Regenerative:

Regenerative heat exchangers have both the fluids travelling within the same channel in counter flow directions. The heat from one fluid is stored in a thermal storage medium before being transferred, which is done by allowing both the fluids to wash the same surface area of the thermal storage medium. There are two types of regenerative heat exchangers, Fixed Matrix and Rotary regenerators. The former has a fixed matrix used as the thermal storage medium on which a periodic and alternating flow of hot and cold fluid is passed to achieve heat exchange. The rotary heat exchanger consists of heat storage matrix in form of rotary devices such as a drum made of metal plates or mesh. The fluids do not meet each other as they flow along all parts of the matrix successively. The rotary regenerative heat exchanger is more efficient in comparison to fixed matrix heat exchanger as the heat transfer surface area is larger due to the rotary property of the heat transfer matrix.

2.1.2. Classification by Heat Transfer Process

Indirect contact:

The flow of both fluids is separated by a partition called as the primary or direct contact surface made of thermal conductive material by which all possibilities of contact between the fluids are nullified. Indirect contact heat exchangers can work in a wide range of temperatures and pressures. A common example of this type of heat exchanger is the shell and tube heat exchanger.

Direct contact:

In direct contact heat transfer, there is an absence of parting wall between the two fluids. Heat transfer is done by physical exchange of thermal energy between the fluids. A major disadvantage with direct contact heat exchanger is that they require both the fluids need to immiscible or in separate phases to avoid mixing. Direct contact heat exchangers are used due to their low construction and maintenance costs. An example of such heat exchangers are cooling towers in power stations.

2.1.3. Classification by Flow Arrangement:

Counter flow:

The flow direction of fluids within the heat exchanger is against each other, which is the most efficient in comparison to other flows. This is because the thermal stresses due to difference in temperature at the cross section are at minimum. This reduced thermal stress on the exchanger wall increases the performance of the heat exchanger. The major disadvantage of counter flow heat exchanger is complexity involved in the design of inlet and outlet headers.

Cross flow:

In this type of heat exchanger, the flow of the fluids is perpendicular to each other. The thermal effectiveness for the crossflow exchanger falls in between those of the parallel flow and counter flow arrangements. The simplicity of inlet and outlet header design involved in crossflow heat exchanger is the reason behind application of this type of heat exchanger. Crossflow heat exchangers are further categorized into mixed and unmixed depending on the contact between the fluids.

Parallel flow:

The fluids in the heat exchanger flow in the same direction. Both the fluids enter at one end and exit through the other together. Though parallel flow heat exchangers have the least efficiency, they have certain advantages. They provide rapid heating to very viscous fluids and reduce pumping requirements in heat exchangers where moderate mean metal temperatures are required on tube walls.

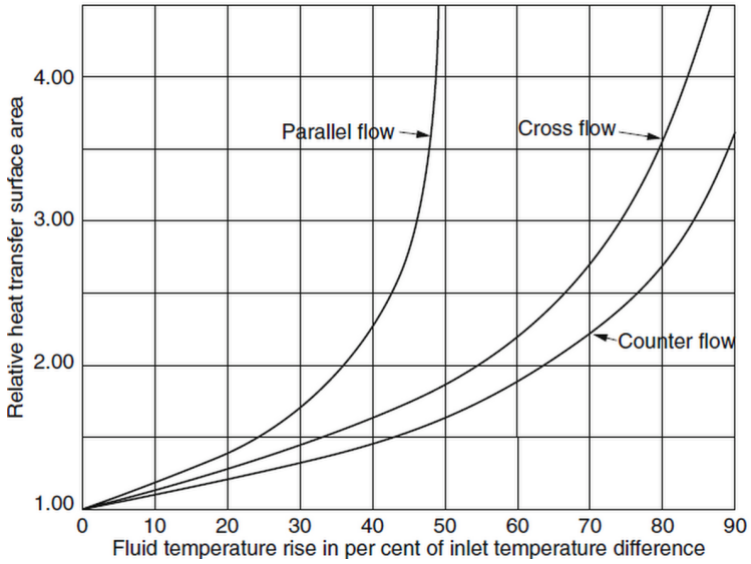

Figure 2-2 : Relative heat transfer area to the difference in temperature to the inlet streams for different flow configurations [8]

The graphical representation of the relative heat transfer surface area vs. the fluid temperature rise of inlet temperature difference in percentage is represented above. From the illustration in counter flow heat exchangers, the temperature difference is very close to the temperature at the inlet, due to which counter flow heat exchanger require the least area in comparison to parallel and cross flow heat exchanger. Whereas in parallel flow heat exchangers there is a small percentage of difference in temperature at the inlet of the fluid to the heat exchanger, hence a larger cross-sectional area is required to generate sufficient heat transfer.

2.1.4. Classification According to Phase of Fluids

The heat exchanger is classified based on the phases of fluids which are further categorized as (1) Gas-Liquid, (2) Liquid-Liquid, (3) Gas-Gas. The most common type of Liquid-Gas heat exchanger is the radiator which cools the engine jacket water by air and this exchanger has tube fin type compact heat exchangers with liquid flowing along the tube side. In this type the enhancement in heat transfer rate is generally achieved by placing the fins outside of the tube. Most of the shell and tube type heat exchangers and some of PHEs comes under the Liquid - Liquid type which has forced convection mode of heat transfer. Heat transfer rate enhancement

is achieved using low-finned tubes, microfin tubes, and heat transfer augmentation devices. Gas-Gas exchanger are larger in size compared to Liquid-Liquid type. This type of exchangers is found mostly in exhaust gas-air preheating recuperators, rotary regenerators, intercoolers or aftercoolers which are used to cool the supercharged engine intake air in some of land-based diesel power packs and in cryogenic gas liquefaction systems. Unlike other two types the use secondary surfaces achieve the heat transfer enhancement.

2.1.5. Classification According to Heat Transfer Mechanisms

Heat transfer from one fluid to the other follows the basic heat transfer mechanisms which are Single-phase convection, free or forced, Two-phase convection either evaporation or condensation by forced or free convection, Convection and radiation combined. All the heat exchangers use these heat transfer mechanisms either individually or in combinations. Depending on the phase change mechanisms, the heat exchangers are classified as condensers and evaporators.

Condensers can be water or air cooled in which the condensing stream heat is used for heating fluid. In water cooled steam condensers the condensing fluid flows outside the tubes and in air cooled steam condensers like in refrigerators or air-conditioners the condensing fluids flows inside. Heat transfer enhancement on the gas side is achieved by providing fins.

Evaporators group of tubular heat exchangers are subcategorized as Fired systems and Unfired systems. Former system is called as Boilers which can be fire tube boiler or a water tube boiler. Latter system follows the steam generation process used in chemical and food processing applications.

2.1.6. Other Classifications of Heat Exchanger

Micro heat exchanger

In micro heat exchanger the fluid flows in lateral confinement through a cavity called microchannel with dimensions of 1 mm below. Due to its smaller and light weight it reduces the supporting structural requirements and increases its mobility. These heat exchangers are commonly used in automotive, aircraft and manufacturing industries.

Printed circuit heat exchanger

In PCHE the flow can be either crossflow or counter flow. Some of the features of the PCHE are its high compactness achieved by its small channel size and it can withstand high temperatures and pressure up to 50 MPa. They can be incorporated more than two process streams to a single unit **[8]**.

Perforated plate heat exchangers

These perforated plate heat exchangers meet the requirements of high efficient compact and cooling systems needed in Cryocoolers. These are made of high thermal conductivity metals of perforated plates in large number are stacked in array with small gaps provided by the spacers. Gas and other stream flows parallel and in opposite direction to each other with other streams flowing through the gaps.

Scraped surface heat exchanger

This heat exchanger is employed in the food, chemical, and pharmaceutical industries in which it prevents the substantial deposition of solid on the surface. This is used mostly in food processing where the characteristics like viscous, sticky and crystallization are likely to be present. Its construction is more of double pipe with process fluid flowing inside and water or steam through the annulus.

Graphite heat exchanger

Due to its high thermal conductivity and high corrosive resistance to many of the chemicals these are used in major industries like chemical, petrochemical, pharmaceutical and metal finishing. Some of the types of this heat exchangers are Cubic heat exchangers, Graphite block heat exchangers, Polytube graphite shell and tube heat exchangers, and Modular-block cylindrical exchanger.

3. Overview of Counterflow Heat Exchanger Analytical Modeling

3.1. Counterflow Heat Exchanger Overview

This section presents an overview of design and analysis of a counterflow helical heat exchanger. Counterflow heat exchangers are used widely in all industrial applications due to their compact structure and higher heat transfer rate than the parallel flow. An initial design geometry was considered and used to analyze straight annular heat exchanger. The initial straight annular heat exchanger without fin is shown in Figure 3-1. The central region of this kind of heat exchangers can be used for locating other internal components and increases the heat transfer surface area by radially increasing the diameter outward.

Three geometric categories of counter flow heat exchanger were considered in analytical model. Cylindrical annular heat exchanger without and with radial fins, annular heat exchanger with helically shaped passage and helical fin heat exchanger with lean angle.

3.2. Assumptions

The one-dimensional analytical modeling of a heat exchanger assumes the following assumptions,

1. Heat exchanger operates in steady state and flow is adiabatic
2. The flow enters the heat exchanger is fully developed in both momentum and thermal profiles
3. Outer and innermost pipe are isolated
4. Zero wall resistance

The heat transfer goals were verified by comparing the required and available heat transfer coefficient. The required and achievable heat transfer coefficient was calculated using the following equations

$$\boldsymbol{q = U_{req} A_s \Delta T_{lm}} \quad (1)$$

Where the q is heat transfer rate, A_s is the heat transfer surface area, U_{req} is the overall heat transfer coefficient which is required to achieve the desired heat exchange,

$$\boldsymbol{U_{ach}} = \left(\frac{\mathbf{1}}{\boldsymbol{h_h}} + \frac{\mathbf{1}}{\boldsymbol{h_c}}\right)^{-\mathbf{1}} \tag{2}$$

In heat exchanger analysis the fluid pressure drop is an important parameter and it was calculated by the equation shown below,

$$\Delta \boldsymbol{P} = \frac{\boldsymbol{f L \dot{m}}}{\mathbf{2}\boldsymbol{\rho D_h A_{crs}}^{\mathbf{2}}} \tag{3}$$

Where $\boldsymbol{f}$ is the frictional factor, $\boldsymbol{L}$ is the length of the channel, $\boldsymbol{\dot{m}}$ is the mass flow rate of the fluid, $\boldsymbol{\rho}$ is the density of the fluid, $\boldsymbol{D_h}$ is the hydraulic diameter of the pipe and $\boldsymbol{A_{crs}}$ is the cross-sectional area of the channel. There were different frictional factor correlations was used for different types of heat exchangers.

The following subsection shows the Nusselt number and frictional factor correlations used in analytical modeling of counter flow straight and helical fin heat exchanger.

3.3. Straight Annular Heat Exchanger Without and With Radial Fins:

Heat exchanger performance can be improved by choosing higher thermal conductivity working fluids or increase the heat exchanger surface area or altering the orientation of the channel and altering the geometry. In his study the heat exchanger performance was improved by increasing the heat transfer surface area by radial fins.

To increase the heat exchanger performance straight radial fins were included between the mid pipe and outer pipe as well as innermost pipe. The heat exchanger without radial fins and with straight radial fins are shown below in Figure 3-1 and 3-2.

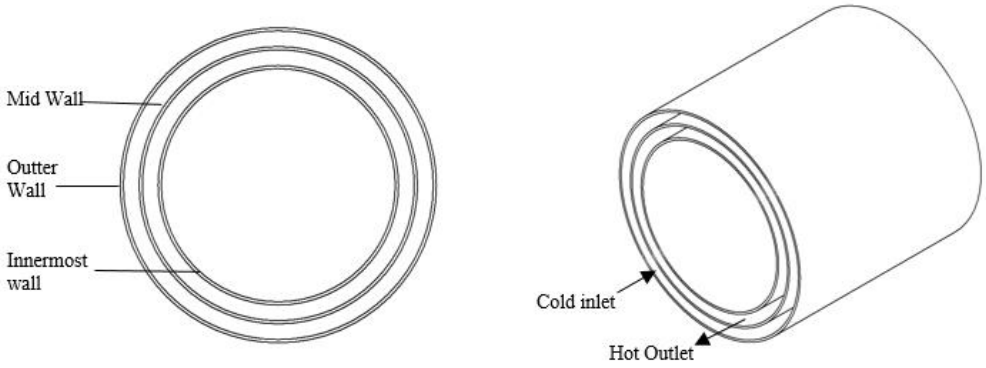

Figure 3-1: Straight annular heat exchanger without fin

The Nusselt number and frictional correlations which were used and valid for straight channels are shown below,

The flow is laminar and $\mathbf{Pr \geq 0.6}$ then Nusselt number is given by equation 4,

$$\boldsymbol{Nu_D = 4.36} \tag{4}$$

The frictional factor for laminar flow regime is given by equation 5 and Colebrook-white equation is used for turbulent regime as shown in equation 6,

$$\boldsymbol{f_s} = 64/\boldsymbol{Re_D} \tag{5}$$

$$\frac{\mathbf{1}}{\sqrt{\boldsymbol{f_s}}} = -\mathbf{2}\log_{10}\left[\frac{\in/\boldsymbol{D_h}}{\mathbf{3.7}} - \frac{\mathbf{2.51}}{\boldsymbol{Re_D}\sqrt{\boldsymbol{f_s}}}\right] \tag{6}$$

The correlation shown below is valid for, $\mathbf{3,000 \leq Re_D \leq 5x10^6}$, $\mathbf{0.5 \leq Pr \leq 2,000}$ and $\mathbf{L \geq 10D_h}$. Darcy frictional factor was considered for calculating the frictional factor for straight channels and its shown in equation 8,

$$\boldsymbol{Nu_D} = \frac{(\boldsymbol{f/8})(\boldsymbol{Re_D} - \mathbf{1000})\boldsymbol{Pr}}{\mathbf{1 + 12.7}(\boldsymbol{f/8})^{0.5}(\boldsymbol{Pr}^{2/3} - \mathbf{1})} \tag{7}$$

$$\boldsymbol{f} = (\mathbf{0.790}\boldsymbol{ln Re_D} - \mathbf{1.64})^{-2} \tag{8}$$

The heat exchanger performance was evaluated between straight annular without fin and with radial fins having same geometrical parameter, for the mass flow rates of hot and cold fluids are 0.01 kg/s and 1 kg/s respectively. It's been reported that the pressure drop increased by 20% than the initial counter flow heat exchanger with no fins while the heat transfer coefficient ratio of straight annular heat exchangers with radial fins achieved 2% more than the without fin heat exchanger.

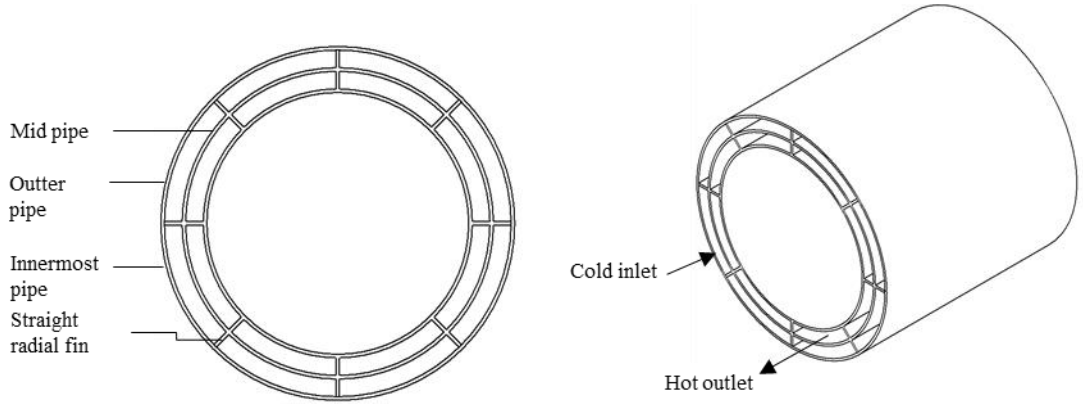

Figure 3-2 : Straight annular heat exchanger with radial fin

However, the ratio of require to achievable heat transfer coefficient was increased by introduced helically shaped passage heat exchanger.

3.4. Helical Annular Heat Exchanger With Radial Fins

In literature, it has been widely reported that the heat transfer rate of helical coil are higher as compared with straight tubes. A schematic view of helical annular heat exchanger with 8 fins is shown in Figure 3-3. The helical passages were characterized by the number of turns, N, over the length of the heat exchanger, L, or Helical angle, ψ.

Dean Number was introduced to analyze the secondary flow within the passage of the helical heat exchanger. The centrifugal force caused due to the curvature of the coiled heat exchanger has been studied by J.S. Jayakumar **[4]** and it has been stated that the centrifugal force causes the secondary flow, hence the heat exchange increases. There were different correlations considered to obtain the local Nusselt number on helical coil heat exchangers.

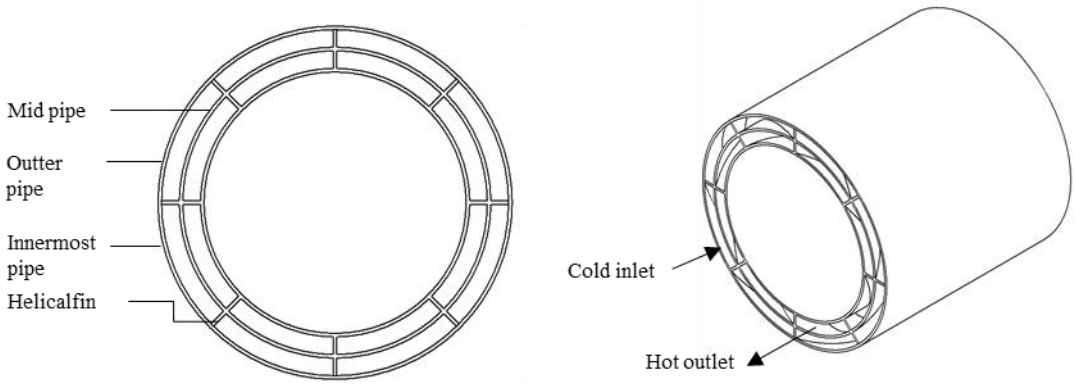

Figure 3-3 : Front view and isometric view of helical fin heat exchanger

The critical Reynolds number, was used to identify the transition from laminar to turbulent flow in curved or helical pipes, is calculated as shown in equation (10) and the Dean number is shown in equation (9),

$$De = Re_D(a/R)^{1/2} \tag{9}$$

$$Re_{crit} = 2100\left[1 + 12(R/a)^{-0.5}\right] \tag{10}$$

The following Nusselt number and frictional correlations were used to model the helically shaped passage heat exchanger. For helical coils with constant heat flux, the Nusselt number has been developed by Manlapaz and Churchill **[10]** for laminar fully developed flow and is given by equation (31). Nusselt correlations for turbulent flow developed by Schmidt is suggested for $2x10^4 < Re < 1.5x10^5$ and $5 < R/a < 84$ and is given by equation (34). For low Reynolds number Pratt's correlation is recommended and is for $1.5x10^3 < Re < 2x10^4$and is given by equation (35).

$$Nu_{cv} = \left[\left(4.364 + \frac{4.636}{x_3}\right)^3 + 1.816\left(\frac{De}{x_4}\right)^{3/2}\right]^{1/3} \tag{11}$$

$$x_3 = \left(\left(1 + \frac{1342}{De^2 Pr}\right)\right)^2 \tag{12}$$

$$x_4 = 1 + \frac{1.15}{Pr} \tag{13}$$

$$Nu_{cv} = Nu_s \left[1 + 3.6\left[\left(1 - \frac{a}{R}\right)\right]\left(\frac{a}{R}\right)^{0.8}\right] \quad (14)$$

$$Nu_{cv} = Nu_s \left[1 + 3.4\left(\frac{a}{R}\right)\right] \quad (15)$$

In the above expressions, Nu_{cv} is the Nusselt number for curved or helical pipes and Nu_s is the Nusselt number for straight pipes. In helical coils, the flow generally becomes fully developed within the first half turn of the coil. The required and achievable convective heat transfer coefficient is calculated using equation (1) and (2). Frictional factor for a fully developed laminar flow in helical coil proposed by Manlapaz and Churchill [] is given by equation (16)

$$\frac{f_{cv}}{f_s} = \left[\left(1 - \frac{0.18}{[1 + (35/De)^2)]^{0.5}}\right)^m + \left(1 + \frac{a/R}{3}\right)^2 \left(\frac{De}{88.33}\right)\right]^{0.5} \quad (16)$$

In the above equation f_c is the frictional factor for curved pipes, f_s is the frictional factor for straight pipes, m = 2 for De < 20; m =1 for 20 < De < 40; and m = 0 for De > 40. Appropriate f_s can calculated based on Re_D. Turbulent flow frictional factors as shown in equation (17) was developed by Srinivasan and can be used when $Re\left(\frac{R}{a}\right)^{-2} < 700$ and $7 < \frac{R}{a} < 104$.

$$f_{cv}\left(\frac{R}{a}\right)^{0.5} = 0.084\left[Re\left(\frac{R}{a}\right)^{-2}\right]^{-0.2} \quad (17)$$

3.5. Helical Annular Heat Exchanger With Radial Fins and Lean Angle

The geometry shown in Figure 3-4 represents a highly compact and efficient device, however, the geometry cannot be fabricated using 3D printing because there is no way to build-up the helical passage walls due to them being cantilevered perpendicular from the wall without support. To amend this issue, a lean angle is used during the build. A schematic of the heat exchanger with 8 channels in the cold section and 4 channels in the hot section with fins having a lean angle is shown in Figure 3-3.

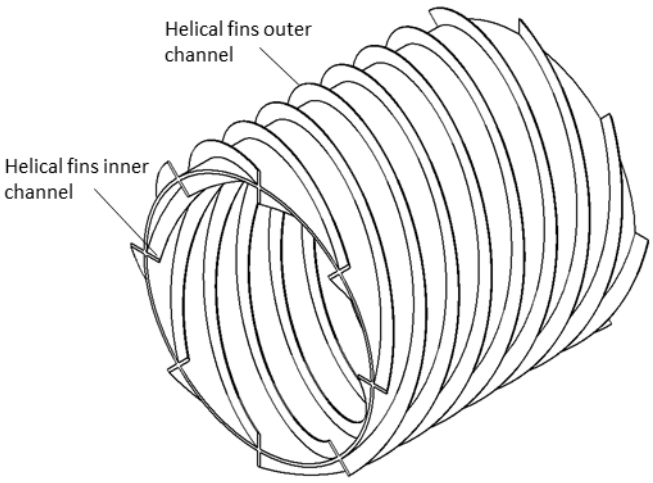

Figure 3-4 : Computational domain of the helical fin heat exchanger

In case of radial fins with a lean angle, Θ the area of the channel remains the same, but the wetted perimeter changes when compared to those of the model without lean. Thus, the hydraulic diameter changes and varies the Reynolds number and thus ultimately changing the achievable overall heat transfer coefficient. The frictional factor and the Nusselt number correlation are the same to that of the helical coils without lean. Figure 3-5 shows that the 3D printed helical heat exchanger with lean angle of 45^0 .

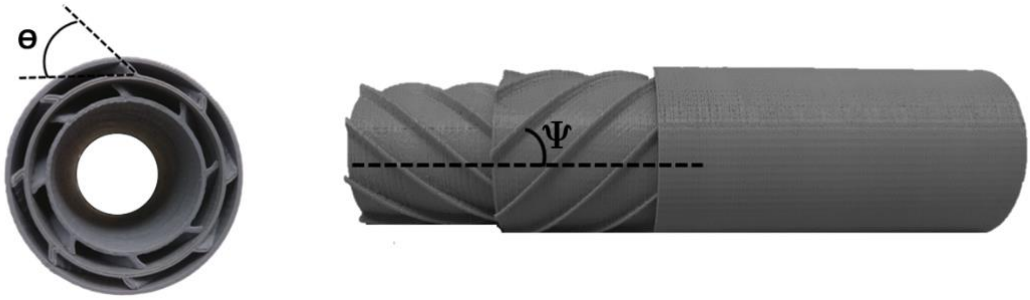

Figure 3-5 : 3D printed helical fin heat exchanger

3.6. Geometry Implications

In Table 3-1, in the straight channel case (Θ = 0°, N = 0, Ψ = 90°), L, Acrs, and P are normalized to 1 for comparison. As N increases, Ψ increases, Lhlx increases, and Acrs and P decrease for a fixed Length and Diameters. When a lean angle, θ is introduced, L and Acrs do not change, however P increases thus decreasing Dh. In helical case there is an increase in length and also increases the pressure drop across the heat exchanger. Increasing the number of turns will result in higher heat transfer rate, but also a higher pressure drop.

Figure 3-6 shows change in helical angle when heat exchanger length is varied for a fixed number of helical turns (in this case, N = 1). In figure 3-6, as heat exchanger length increases for a fixed N, the helical angle increases which in turn decrease the cross-sectional area and perimeter.

Table 3-1 : Summary of important heat exchanger geometric parameters

Parameters	**Θ = 0º**				**Θ = 45º**			
	N = 0	**N = 0.5**	**N = 1**	**N= 1.25**	**N = 0**	**N = 0.5**	**N = 1**	**N = 1.25**
Ψ	90	50.57	31.4	22.1	90	50.7	31.4	22.1
L_{hlx}	1	1.29	1.92	2.66	1	1.29	1.92	2.66
A_{crs}	1	0.77	0.51	0.37	1	0.77	0.51	0.37
P	1	0.78	0.54	0.40	1.02	0.80	0.56	0.42
D_h	1	0.98	0.95	0.91	0.98	0.96	0.92	0.86

Figure 3-7 shows change in number of helical turns, N when heat exchanger length is varied for a fixed helical angle (in this case, Ψ = 31.4° (calculated for N = 1)). In figure 3-7, as heat exchanger length increases for a fixed Ψ, number of helical turns increases too, but there is no change in cross sectional area and perimeter.

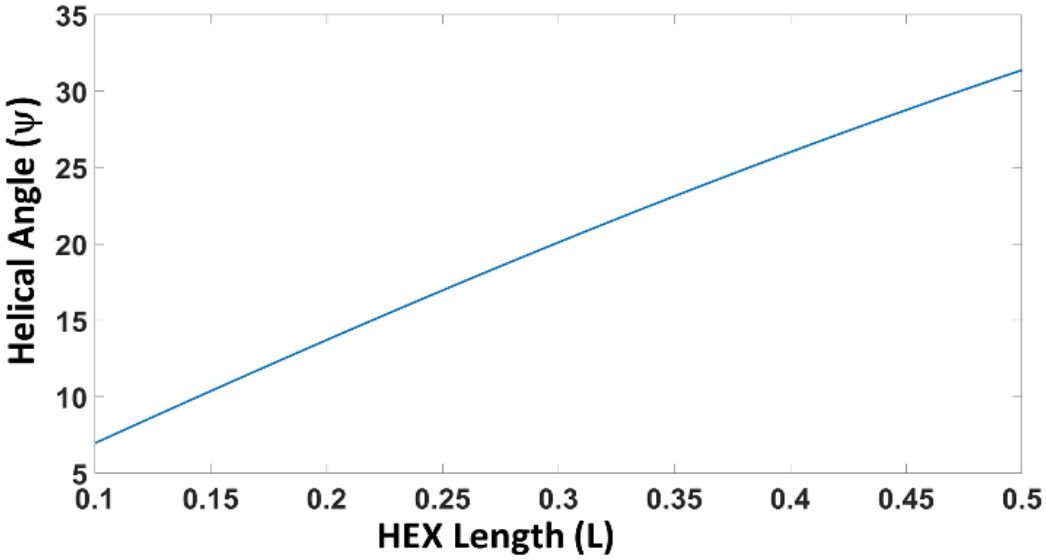

Figure 3-6 : Helical angle X vs heat exchanger length for fixed N =1

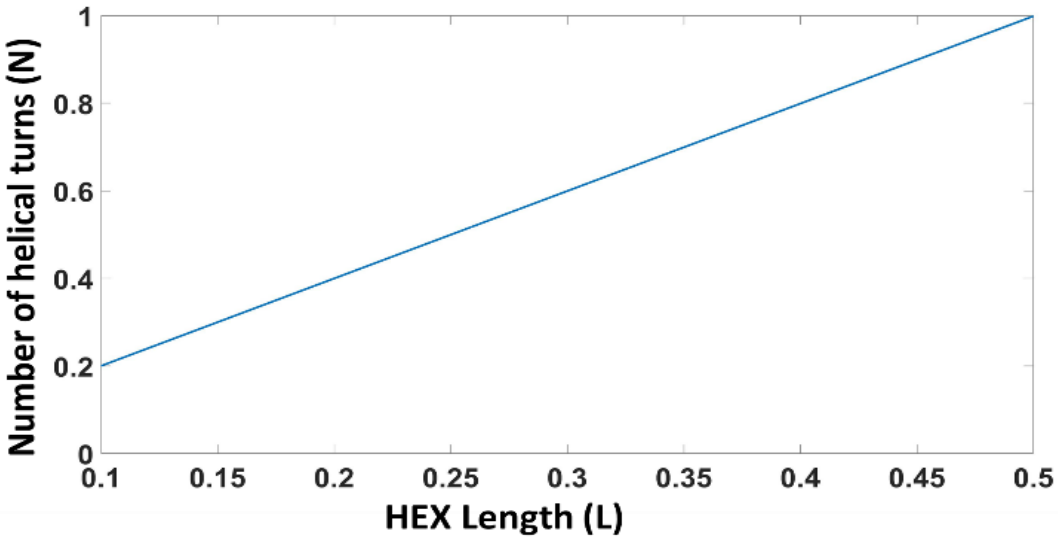

Figure 3-7 : Number of helical turns, N vs heat exchanger length (L) for fixed X = 24.4^0

3.7. Important Results from 1-D Analytical Model

This section presents the performance for the various heat exchanger geometries discussed above. The geometric constraints and flow conditions are summarized in Table 3-2.

The constraints are set by the heat exchanger necessitated performance, variable parameters can be adjusted to achieve required performance. The heat exchanger thermal performance is compared with the resulting pressure drop of the working fluids. The working fluid is water. The objective is to cool the incoming hot fluid (hot water) from 368 K to 298 K using cold fluid (cold water) which enters the heat exchanger at 278 K. Both fluids enter the heat exchanger with static pressure of 202 kPa.

Table 3-2 : Heat exchanger performance parameters

Parameter description	Value or Range	Type
Outer diameter, D_0	$\leq$ 0.28 m	Constraint
Length, L	$\leq$ 0.5 m	Constraint
U_{ratio}	= 1	Constraint
Pressure drop, ΔP	$\leq$ 5 % of Inlet pressure	Constraint
Hot fluid inlet temperature, $T_{h,i}$	368 K	Constraint
Hot fluid exit temperature, $T_{h,o}$	298 K	Constraint
Cold fluid inlet temperature, $T_{c,i}$	278 K	Constraint
Wall and fin thickness, t_o, t_i, t_f	-	Variable
Hot fluid mass flow rate, $\dot{m}_h$	0.01 kg/s – 0.1 kg/s	Desired operating range
Cold fluid mass flow rate, $\dot{m}c$	0.1 kg/s – 1 kg/s	Desired operating range
Number of turns	-	Variable
Fluid	Water	Constraint

For the initial analysis D_0 = 0.28 m, C_{hi}= 0.005 m, C_{ho}= 0.005 m, L = 0.5 m, and the fin and wall thickness are all 0.001 m. The energy balance and log mean temperature difference are used to find the heat transfer rate or the power required to lower the temperature of the hot fluid and find the exit temperature of the cold fluid. U_{ratio} and U_{ach} for different fluid mass flow rates

are calculated. The following subsections presents the performance results of the various heat exchanger geometries and configurations.

3.7.1. Results for Straight Annular Heat Exchanger Without and With Radial Fins

Table 3-3 shows the heat exchange (q), Cold fluid exit temperature (Tc,o), Ureq, Uach and U_{ratio} variation for different mass flow rate combinations in a straight heat exchanger without radial fins.

Table 3-3 : Summary of cases for straight heat exchanger without fin

$\dot{m}_h$ (kg/s)	$\dot{m}_c$ (kg/s)	q (kW)	$T_{c,o}$ (K)	U_{req} (kW/ m^2 K)	U_{ach} (kW/ m^2 K)	U_{ratio}
0.1	0.1	30.3	351	3.917	0.150	0.04
0.1	1	30.3	286	1.650	0.129	0.08
0.01	0.1	3	286	0.165	0.128	0.78
0.01	1	3	279	0.156	0.133	0.85

In case of a straight heat exchanger without fins, U_{ratio} is less than 1 for different mass flow rate cases. This means the hot fluid is not cooled to the desired temperature for this design. To improve the ratio and to achieve the required drop in temperature for the hot fluid, fins are employed, which increases the heat transfer area. Table 3-4 summarizes changes in U_{ratio} when 8 fins are employed in both the inner and outer channel. Heat exchange and the exit temperature of the cold fluid remains the same.

In case of straight heat exchanger with fins, a marginal increase in U_{ratio} is seen when compared to the heat exchanger geometry with no fins. The improvement in U_{ratio} is not significant enough to cool down the hot fluid to the desired temperature.

Table 3-4 : Uratio for straight annular heat exchanger with 8 radial fins in both the channels

ṁh (kg/s)	ṁc (kg/s)	U_{ratio}	Lreq (m) to achieve $U_{ratio} = 1$
0.1	0.1	0.04	12.5
0.1	1	0.08	6.2
0.01	0.1	0.81	0.62
0.01	1	0.88	0.57

In case of straight heat exchanger with fins, a marginal increase in U_{ratio} is seen when compared to the heat exchanger geometry with no fins. The improvement in U_{ratio} is not significant enough to cool down the hot fluid to the desired temperature. In table 4, L_{req} is the heat exchanger length required to achieve $U_{ratio} = 1$ while keeping other geometric parameters the same. For example, to achieve a $U_{ratio} = 1$ operating at ṁh = 0.01 kg/s and ṁc = 1 kg/s the heat exchanger length must be increased to 0.5 m from 12.5m while keeping the rest of the geometric parameters the same. Apart from increasing the length, $U_{ratio} = 1$ can be achieved by varying other geometrical parameters and is discussed in the next section. The frictional pressure loss in a straight heat exchanger with radial fins and without radial fins is summarized in Table 3-5.

Table 3-5 : Frictional pressure drop in a straight annular heat exchanger

$\dot{m}_h$ (kg/s)	$\dot{m}_c$ (kg/s)	ΔP for HEX without fins (kPa)		ΔP for HEX with fins (kPa)		ΔP for L_{req} (kPa)	
		Hot	Cold	Hot	Cold	Hot	Cold
0.1	0.1	0.002	0.002	0.002	0.003	0.05	0.066
0.1	1	0.002	0.048	0.002	0.053	0.03	0.66
0.01	0.1	0.0002	0.005	0.0002	0.005	0.0003	0.006
0.01	1	0.0002	0.056	0.0002	0.062	0.003	0.07

There is an increase in U_{ratio} for the heat exchanger design with fins when compared to the model without fins, however the pressure loss is higher. A long heat exchanger might satisfy U_{ratio} and pressure drop constraints, however the design is not suitable if weight and volume compactness are considered. An improved design is needed to bring the U_{ratio} to 1 and thus we go for a helically coiled heat exchanger. In conclusion, for the initial straight heat exchanger geometry with and without fins, $U_{ratio} < 1$ i.e. the hot fluid does not cool down to the desired temperature.

3.7.2. Results for Helical Annular Heat Exchanger with Radial Fins and no Lean Angle

Helically coiled heat exchangers offer advantages over conventional shell and straight tube heat exchangers in terms of heat transfer rates. It accommodates a large heat transfer area in a small space, with high heat transfer coefficients. Tubes are wrapped around cylinder in a helical shape and number of turns or helical angle are varied which changes the length of the heat exchanger and ultimately the heat transfer area. Due to helical shape a secondary flow (centrifugal force) is created within the channel and allows for better mixing which leads to better heat exchange and thus a higher Uratio. Table 3-6 below showcases how Uratio changes with increasing coil turns in a helical annular heat exchanger having radial fins with no lean.

Table 3-6 : Uratio for helical annular heat exchanger with radial fins having no lean

$\dot{m}_h$ (kg/s)	$\dot{m}_c$ (kg/s)	U ratio		
		N = 0.5	N = 1	N = 2
0.1	0.1	0.08	0.09	0.10
0.1	1	0.20	0.29	0.37
0.01	0.1	1.15	1.27	1.54
0.01	1	1.40	1.88	2.56

Table 3-6 shows Uratio is high for helical heat exchanger when compared to a straight heat exchanger (Table 3-4). Increase in turns gives higher Uratio. As number of turns increases the cross-sectional area of the passages decreases which increases the flow velocity and Reynolds number. Flow is more turbulent when turns are increased and thus there is better mixing which

leads to higher Nusselt number and ultimately better heat transfer. In few mass flow rate combinations, U_{ratio} exceeds 1 and it means that the hot fluid is getting overcooled, i.e. beyond the desired temperature. In such situations either the geometry can be changed to bring it down to 1 or the mass flow rate of hot fluid can be increased, or mass flow rate of cold fluid can be decreased.

3.7.3. Results for Helical Annular Heat Exchanger with Radial Fins and Lean Angle

Due to build constraints, the fins in the heat exchanger are at a lean angle and the table below summarizes how U_{ratio} changes with and without lean for N = 1. When Θ = 90° it means the fins are straight, i.e. no lean and Θ= 45°, means there is a lean angle of 45°.When compared to the case without lean (Θ = 90°), the one with lean (Θ = 45°) increases the U_{ratio} marginally.

Table 3-7 : U ratio comparison for helical annular heat exchanger with Θ = 90^0 and Θ = 45^0, N = 1

$\dot{m}_h$ (kg/s)	$\dot{m}_c$ (kg/s)	U ratio	
		Θ = 90^0	Θ = 45^0
0.1	0.1	0.09	0.09
0.1	1	0.29	0.29
0.01	0.1	1.27	1.30
0.01	1	1.88	1.91

Table 3-8 : Frictional pressure drop in a helical annular heat exchanger for multiple helical turns, N

$\dot{m}_h$ (kg/s)	$\dot{m}_c$ (kg/s)	ΔP (kPa)							
		N = 0.5, Θ = 90°		N = 1, Θ = 90°		N = 1, Θ = 45°		N = 2, Θ = 90°	
		Hot	Cold	Hot	Cold	Hot	Cold	Hot	Cold
0.1	1	0.005	0.007	0.014	0.018	0.015	0.019	0.065	0.082
0.01	0.1	0.006	0.232	0.016	1.49	0.017	1.543	0.073	10.47
0.01	1	0.0004	0.012	0.001	0.031	0.001	0.033	0.004	0.133
0.01	1	0.0004	0.253	0.001	1.46	0.001	1.51	0.004	10.17

The frictional pressure loss in a helical annular heat exchanger is summarized in table 3-8 for distinctive design cases. Increasing number of turns increases helical passage length, decreases cross sectional area, and thus ultimately increases the pressure loss.

3.7.4. ε-NTU Method:

The effectiveness method or the Number of Transfer Units Method is the most convenient method to find the outlet temperatures of the fluid when the heat transfer coefficient and the inlet temperatures are available. Without using any additional assumption, this method can be easily derived from Logarithmic Mean Temperature Difference (LMTD) method. An advantage of this method is to predict the outlet temperatures without resorting to a numerical iterative solution of a system of nonlinear equations. In this study, the outlet temperatures of the fluids were determined using the heat transfer coefficient determined in 1D analytical calculation. The maximum heat transfer rate can be calculated using the equation (18)

$$\boldsymbol{Q_{max} = c_{min}(T_{h,i} - T_{c,i})} \tag{18}$$

Where $\boldsymbol{c_{min}}$ = $\boldsymbol{c_c}$ or $\boldsymbol{c_h}$, whichever is smaller and $\boldsymbol{Q_{max}}$ is the maximum heat that could be transferred between the fluids per unit time. c = $\boldsymbol{\dot{m}C_p}$, For example $\boldsymbol{c_c}$ = $\boldsymbol{\dot{m}_c C_{p,c}}$

The Number of Transfer Units (NTU) is given by,

$$\boldsymbol{NTU = \frac{UA}{C_{min}}} \tag{19}$$

where U – convective heat transfer coefficient and A is heat transfer Area. The effectiveness of the heat exchanger can be calculated using the following formula given in equation (20),

$$\boldsymbol{\varepsilon = \frac{Q}{Q_{max}}} \tag{20}$$

where $\boldsymbol{\varepsilon}$ is the effectiveness. For counter flow heat exchangers, the equation (21) can be used when the C_r <1 and the when C_r = 1 the relation is given in equation (22) **[8]**,

$$\epsilon = \frac{1-exp[-NTU(1-c_r)]}{1-c_r exp[-NTU(1-c_r)]} \quad (21)$$

$$\epsilon = \frac{NTU}{1+NTU} \quad (22)$$

$$C_r = \frac{c_{min}}{c_{max}} \quad (23)$$

The outlet temperature of the fluids, using the maximum heat exchange and the inlet temperature of the fluid and can be calculated using the equations (24), (25) and (26) **[8]**.

$$Q = Q_{max}\, \varepsilon \quad (24)$$

$$T_{h,o} = T_{h,i} - \frac{Q}{(\dot{m}_h C_{p_h})} \quad (25)$$

$$T_{c,o} = T_{c,i} - \frac{Q}{(\dot{m}_c C_{p_c})} \quad (26)$$

3.8. Parametric Study

This section discusses the parametric study done in one dimensional analytical modeling. The parametric study was carried out by varying several heat exchanger geometry parameters such as heat exchanger length, diameter, inner and outer channel heights, number of turns, number of fins, wall and fin thickness. All the cases were run for the mass flow rates of 0.01 kg/s and 1 kg/s of hot fluid and cold fluid respectively. In all the graphs initial geometry with 0.5 helical turn was used to track the heat exchanger performance. The graphs obtained for the parametric studies are shown below.

Figure 3-8 showcases heat exchanger performance when the length is varied from 0.1 m to 0.5 m. U_{ratio} increases due to an increase in heat transfer area and the ΔP decreases with increase in heat exchanger length.

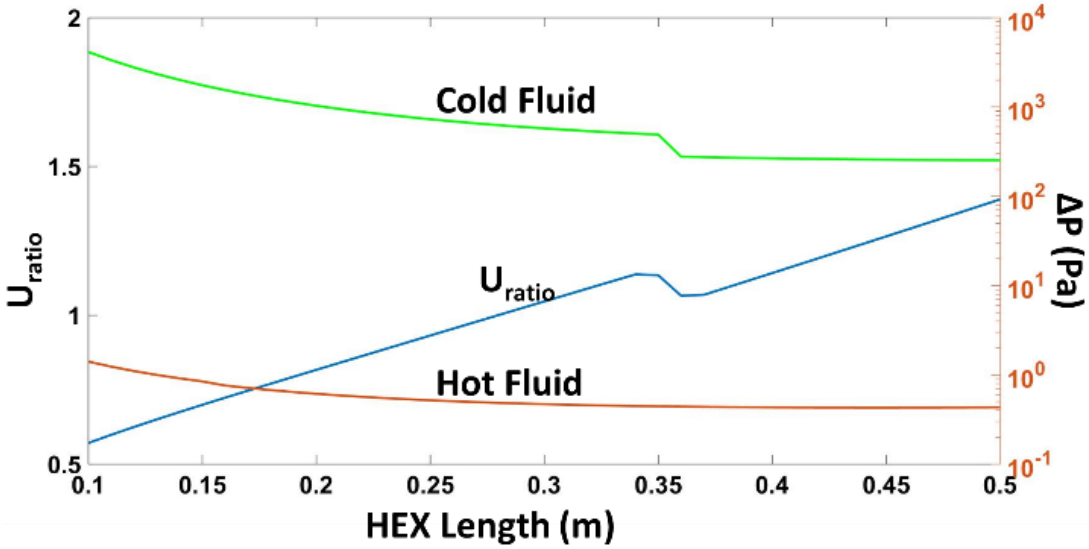

Figure 3-8 : U_{ratio} and ΔP vs Heat exchanger length

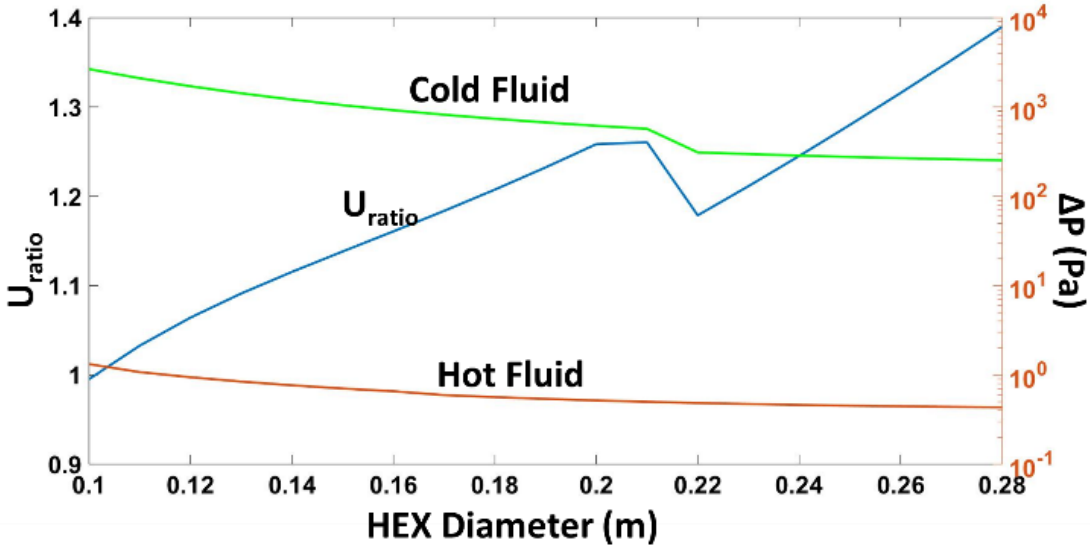

Figure 3-9 : U_{ratio} and ΔP vs Heat exchanger diameter

In Figure 3-9, U_{ratio} (left y axis) and ΔP (right y axis) are tracked when the heat exchanger diameter is varied from 0.1 m to 0.28 m, with the rest of the geometry the same. Increasing diameter increases the heat transfer area and thus increasing the U_{ratio}. A slight change in trend is seen when diameter is 0.21m and it is because there is a change in flow regime, i.e. the flow

changes to laminar from turbulent. Pressure drop decreases in both the channels as the cross-sectional area increases with increase in diameter.

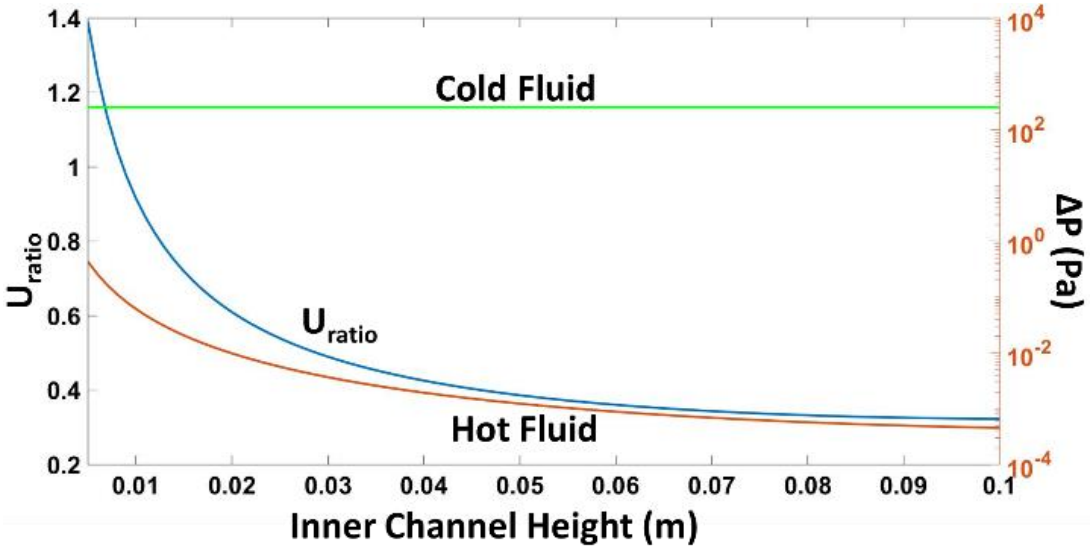

Figure 3-10 : U_{ratio} and ΔP vs Inner channel height

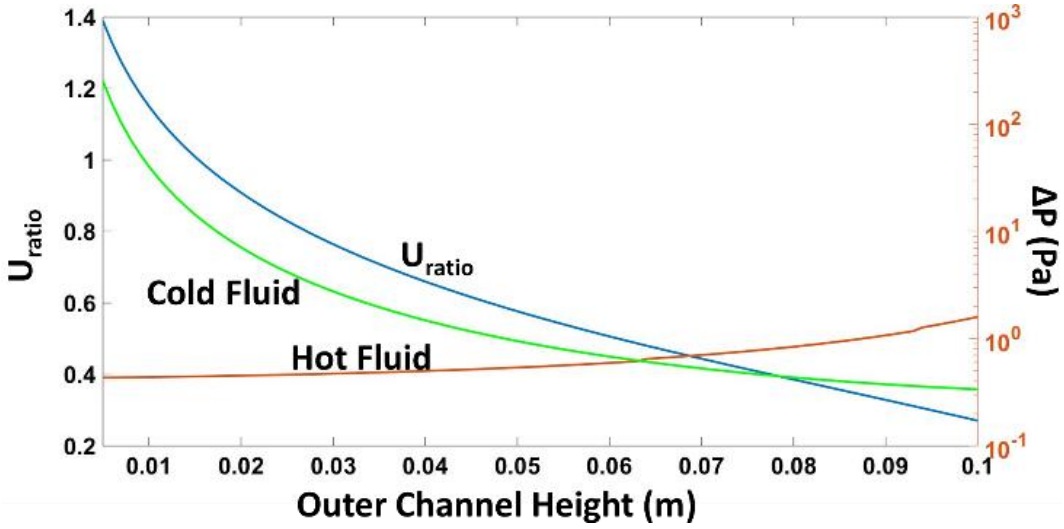

Figure 3-11 : U_{ratio} and ΔP vs Outer channel height

In figure 3-10 and 3- 11, inner and outer channel height is varied and in both the cases Uratio decreases with increase in passage heights. In figure 3-12 and 3-13 the wall and fin thickness have been increased from 0.001 m to 0.01 m and the heat exchanger performance has been tracked

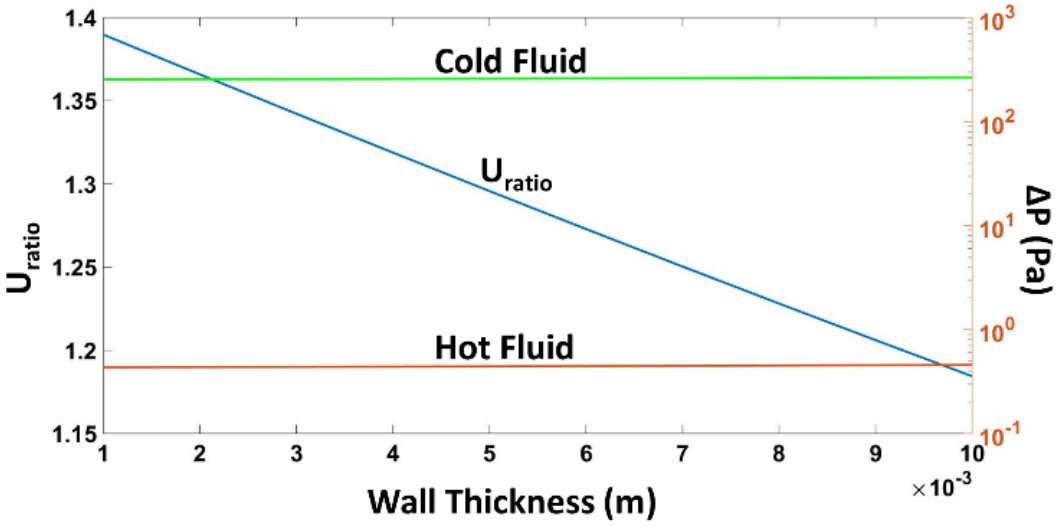

Figure 3-12 : U_{ratio} and ΔP vs Wall thickness

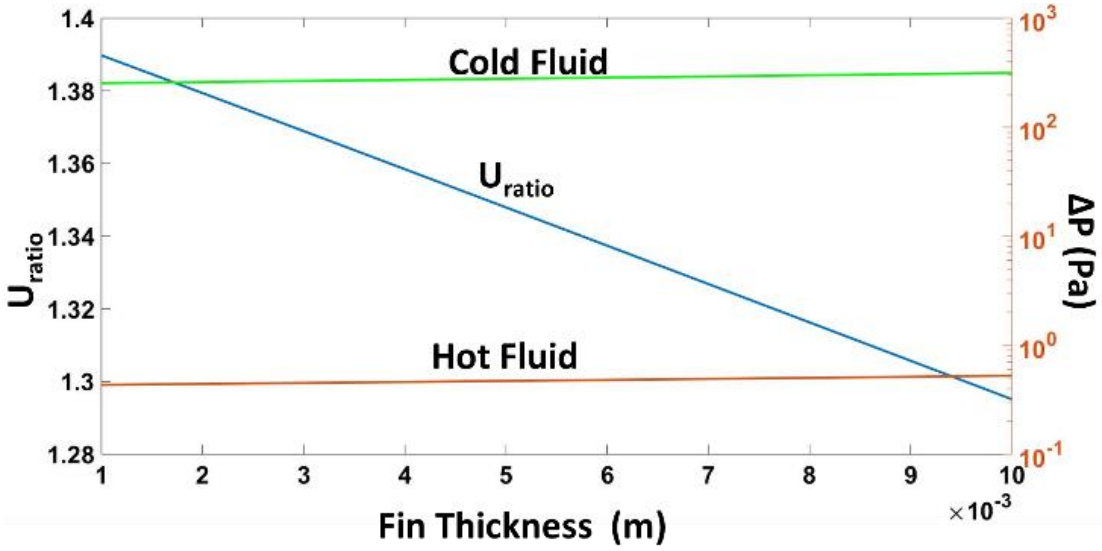

Figure 3-13 : U_{ratio} and ΔP vs Fin thickness

Increasing wall and fin thickness decreases the heat transfer surface area and thus ultimately U_{ratio}. The cross-sectional area of the passages decreases with increase in wall and fin thickness and thus increases the pressure drop in both the passages.

Figure 3-14 summarizes the effects of increasing the number of fins in the fluid passage. Increasing fins increases the heat transfer area and thus U_{ratio}. However more fins mean less cross-sectional area which in turn leads to increase in pressure loss.

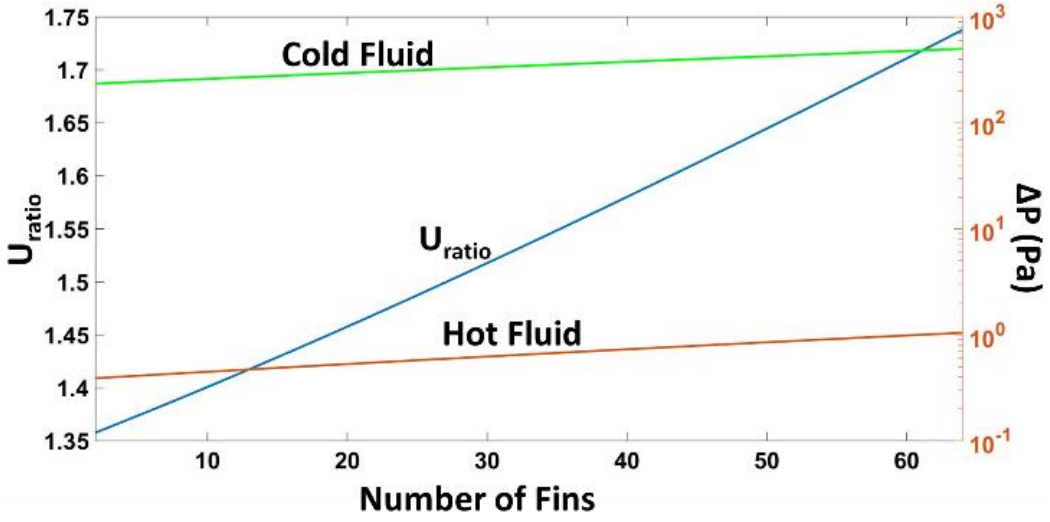

Figure 3-14 : U_{ratio} and ΔP vs Number of fins

In figure 3-15 number of helical turns are increased and this leads to increase in U_{ratio} and ΔP. Increasing helical turns shrinks the cross-sectional area and makes the flow highly turbulent and involves in better mixing. With higher Reynolds number, the Nusselt Number is also high which directly influences leading to higher U_{ratio}. However, we see an increase in pressure loss which comes from decreasing cross sectional area.

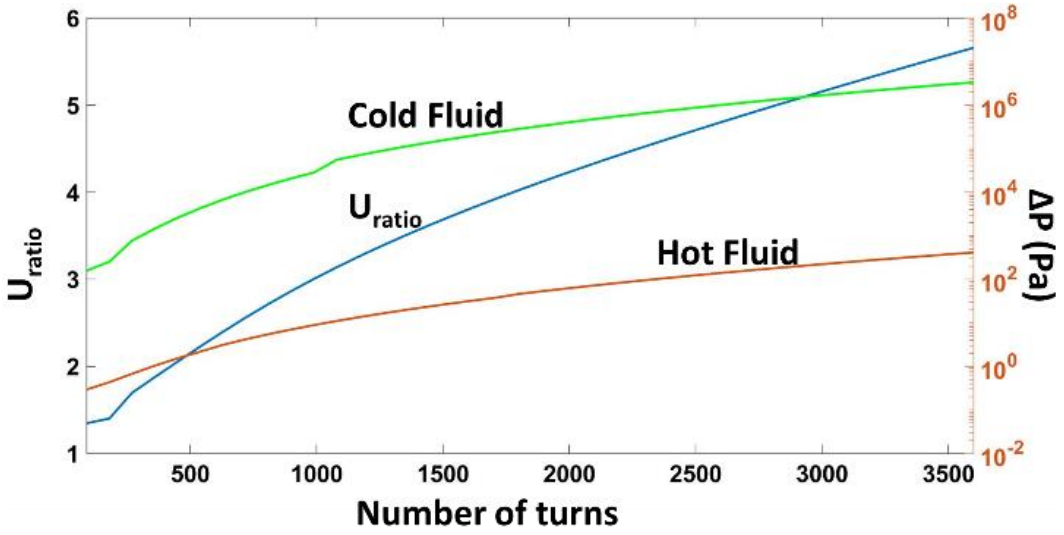

Figure 3-15 : Uratio and ΔP vs Number of turns

3.8.1. Heat Transfer and Compactness Prioritized

This section presents design and performance when heat transfer and compactness are prioritized. The design parameters for water-water heat exchanger are shown in table 3-9. Figure 3-16 and 3-19 illustrates change in U_{ratio} for different mass flow rate combinations for the given mass flow rate range. U_{ratio} equal to 1 can be achieved within the flow rate range. U_{ratio} is equal to one when $\dot{m}_h$ = 0.01 kg/s and $\dot{m}_c$ = 1 kg/s. For cases where U_{ratio} is lesser than 1, mass flow rate of the hot fluid should be decreases or that of the cold fluid must be increases to bring U_{ratio} to 1.

Table 3-9 : Optimized design parameters when heat transfer and compactness are prioritized

Geometry	Length (m)	Diameter (m)	Fin and wall thickness (m)	Channel height (m)		Number of fins		Number of turns	
				Inner	Outer	Inner	Outer	Inner	Outer
1	0.10	0.10	0.001	0.005	0.010	8	8	10	10
2	0.25	0.25	0.001	0.015	0.020	7	7	4	4

Increasing or decreasing mass flow rates to satisfy heat transfer goals means going outside the mass flow rate range. For example, in geometry 1, the mass flow rate of the hot fluid must be decreased to 0.0027 kg/s if the hot fluid flows at 0.1 kg/s to achieve Uratio = 1. It can be seen from the above table that the heat transfer compactness in both the designs are greater than 400 m2/ m3. In terms of mass and volume, Geometry 1 is Preferred.

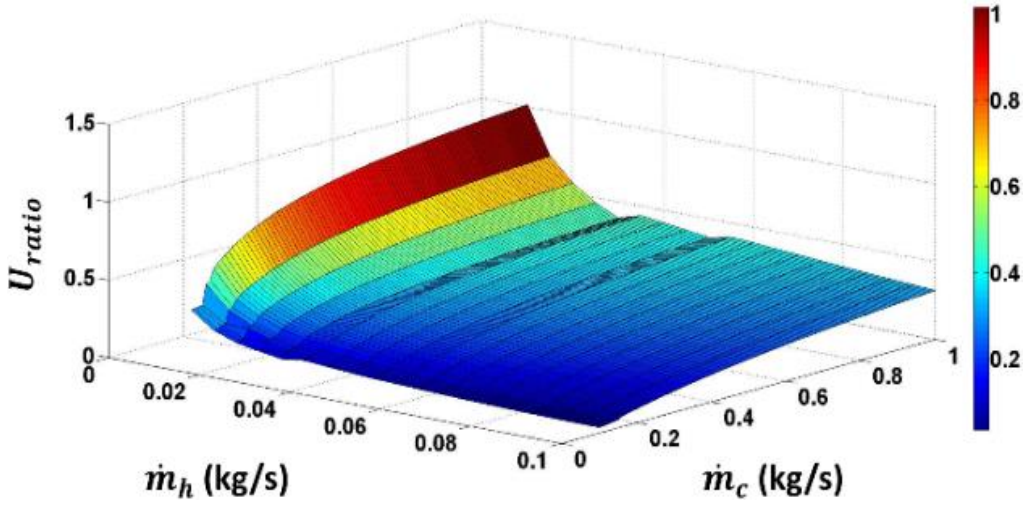

Figure 3-16 : U_{ratio}vs $\dot{m}_h$ vs $\dot{m}_c$ for geometry 1 when heat transfer and compactness are prioritized

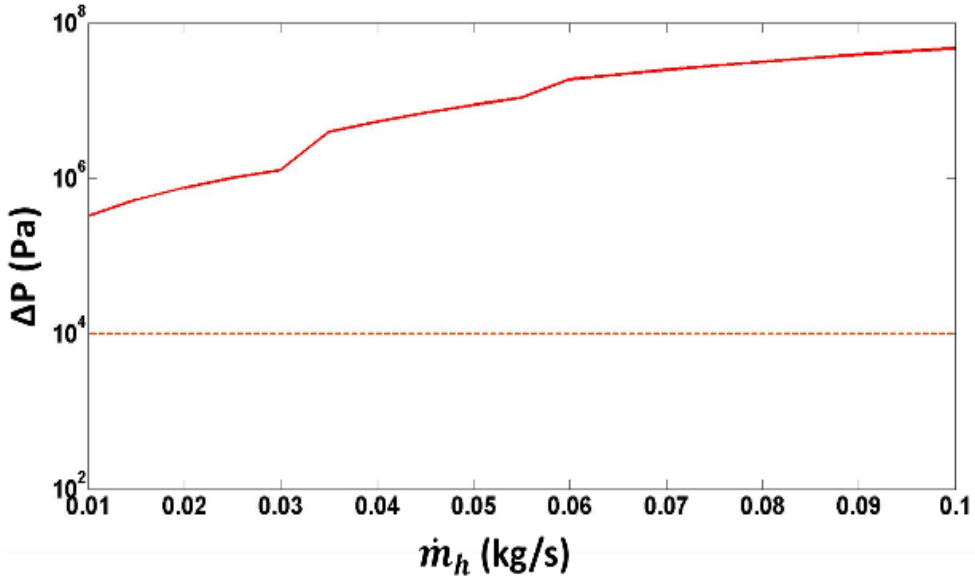

Figure 3-17 : ΔP vs $\dot{m}_h$ for geometry 1 when heat transfer and compactness are prioritized

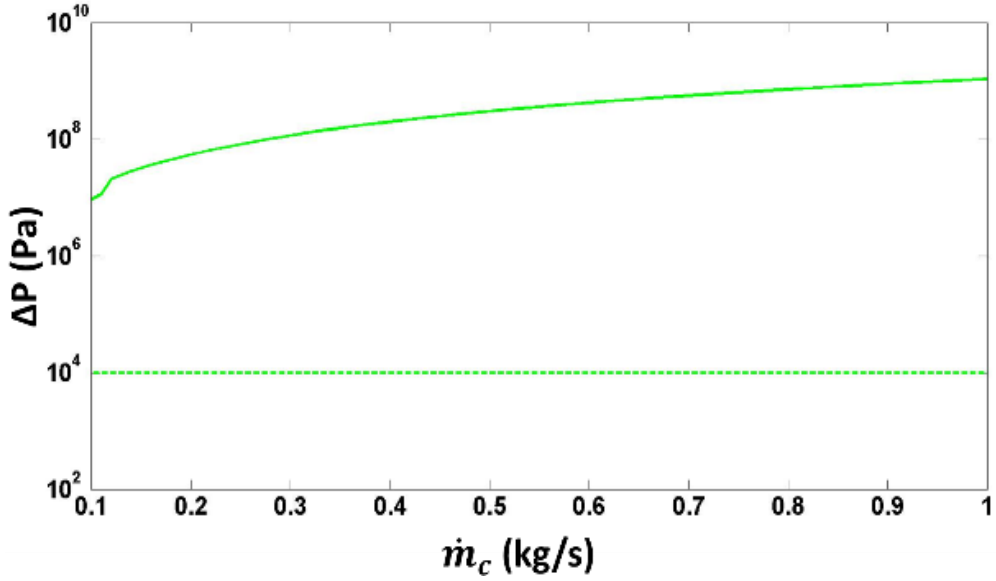

Figure 3-18 : ΔP vs $\dot{m}_c$ for geometry 1 when heat transfer and compactness are prioritized

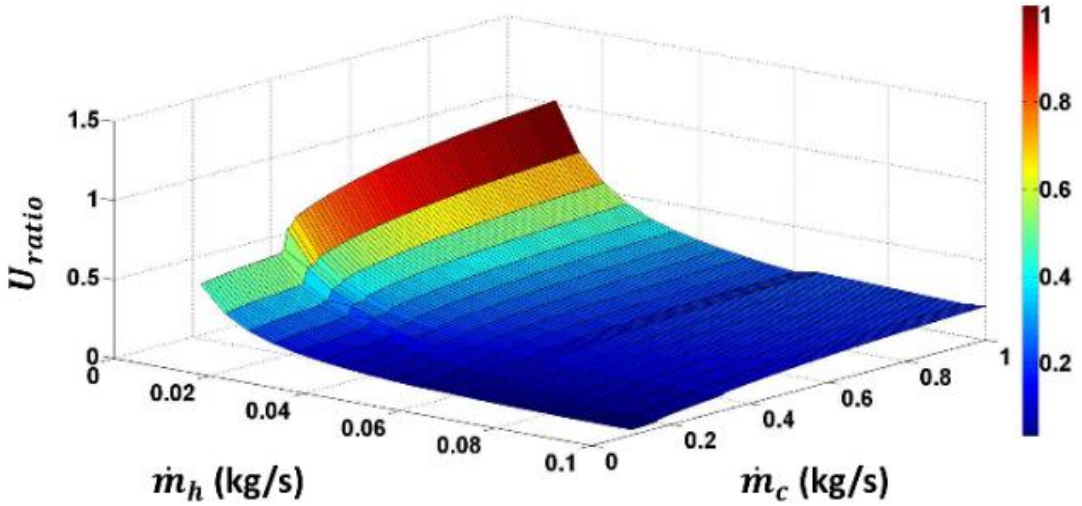

Figure 3-19 : U_{ratio} vs $\dot{m}_h$ vs $\dot{m}_c$ for geometry 2 when heat transfer and compactness are prioritized

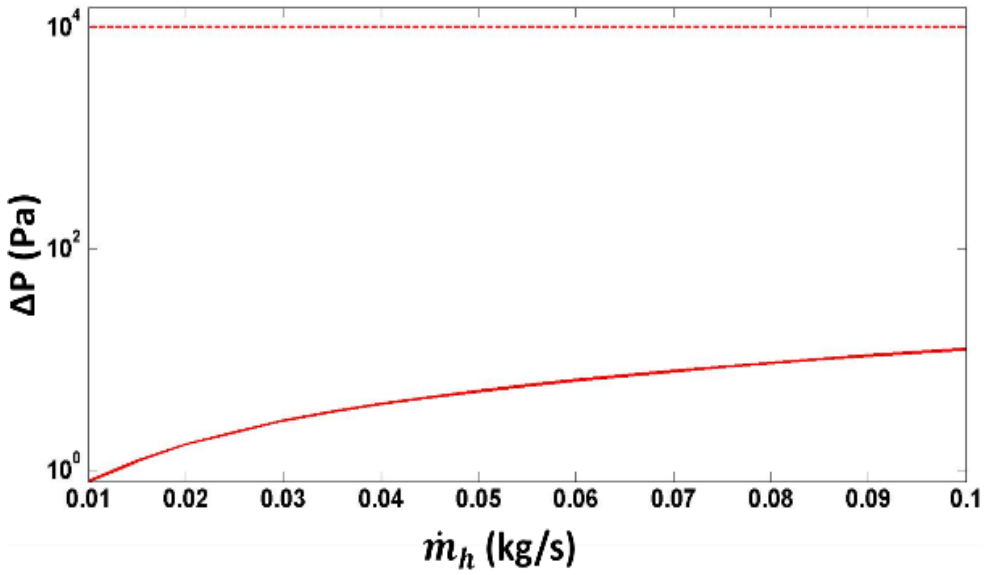

Figure 3-20 : ΔP vs $\dot{m}_h$ for geometry 2 when heat transfer and compactness are prioritized

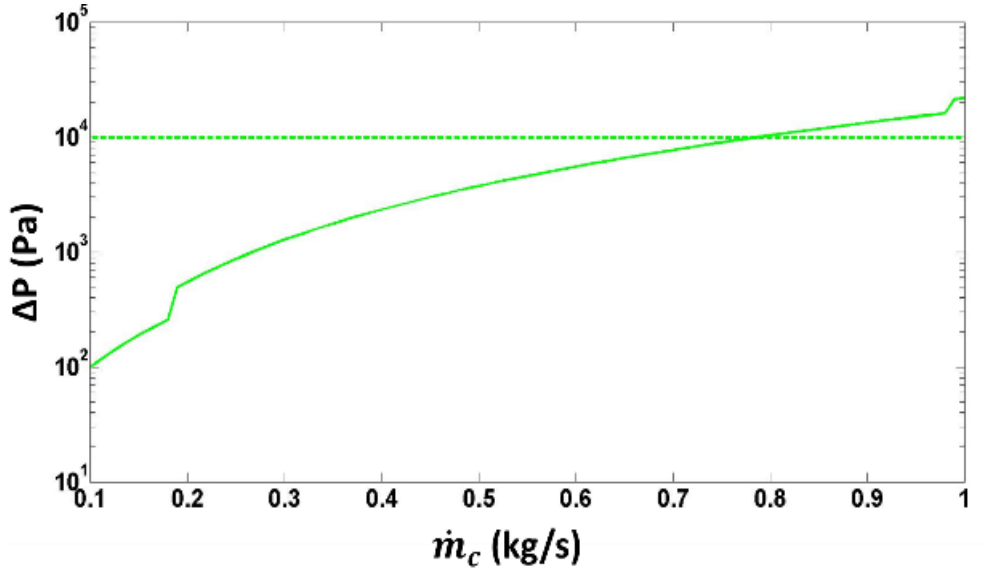

Figure 3-21 : ΔP vs $\dot{m}_c$ for geometry 2 when heat transfer and compactness are prioritized

3.8.2. Pressure Drop and Compactness Prioritized

This section presents a design and its performance when pressure drop and compactness are prioritized. The design parameters for heat exchanger geometries are shown in table 3-10. Figure 3-23, 3-24, 3-26, 3-27 summarizes the pressure drop for heat exchangers design 3 and 4. Pressure drops are within the threshold for the complete mass flow rate range.

Table 3-10 : Optimized design parameters when pressure drop and compactness are prioritized

Geometry	Length (m)	Diameter (m)	Fin and wall thickness (m)	Channel height (m)		Number of fins		Number of turns	
				Inner	Outer	Inner	Outer	Inner	Outer
3	0.10	0.10	0.001	0.022	0.022	2	8	0.5	2.5
4	0.25	0.25	0.001	0.040	0.060	9	9	0.5	2

Figure 3-22 and 3-25 illustrates change in U_{ratio} for different mass flow rate combinations in the given mass flow rate range. U_{ratio} is less than 1 for the entire mass flow rate range and is the main drawback when pressure drop and compactness are prioritized. U_{ratio} can be increased to 1 by either increasing the flow rate of cold fluid or by decreasing the hot fluid mass flow rate.

The better option would be decreasing the mass flow rate of hot fluid as it keeps the pressure drop within the constraints. The volume for design 3 and 4 are 0.0026 m3 and 0.0122 m3 and the mass are 6.99 and 8.68 kg. In terms of mass and volume, Geometry 3 is preferred.

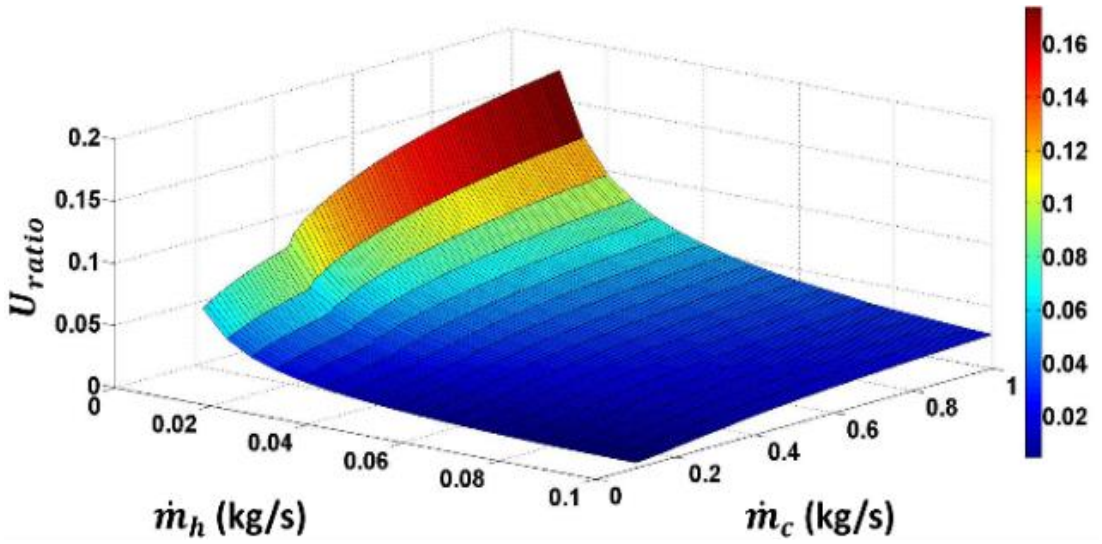

Figure 3-22 : U_{ratio} vs $\dot{m}_h$ vs $\dot{m}_c$ for geometry 3 when pressure drop and compactness are prioritized

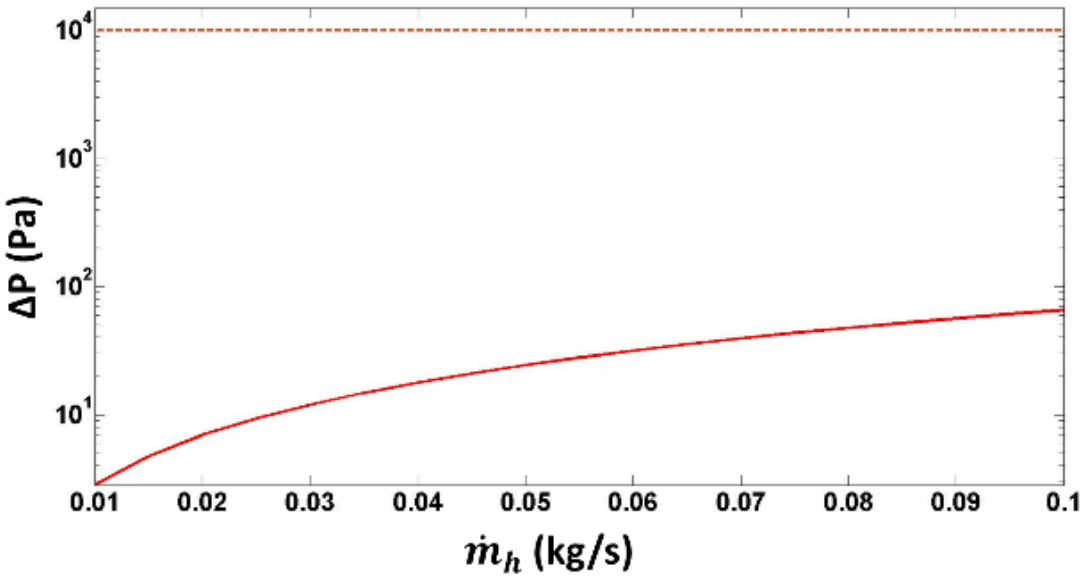

Figure 3-23 : ΔP vs $\dot{m}_h$ for geometry 3 when pressure drop and compactness are prioritized

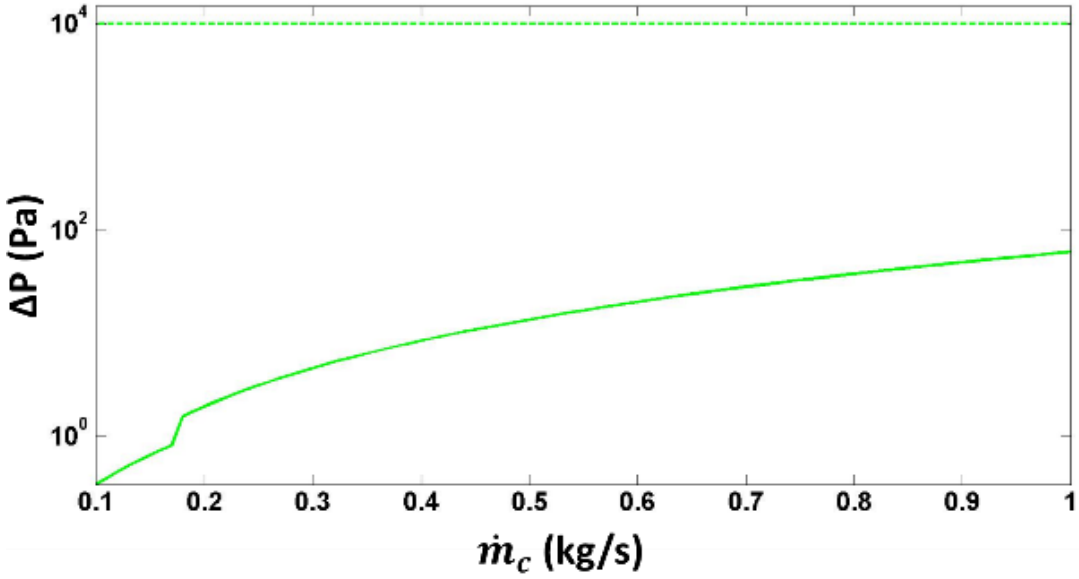

Figure 3-24 : ΔP vs $\dot{m}_c$ for geometry 3 when pressure drop and compactness are prioritized

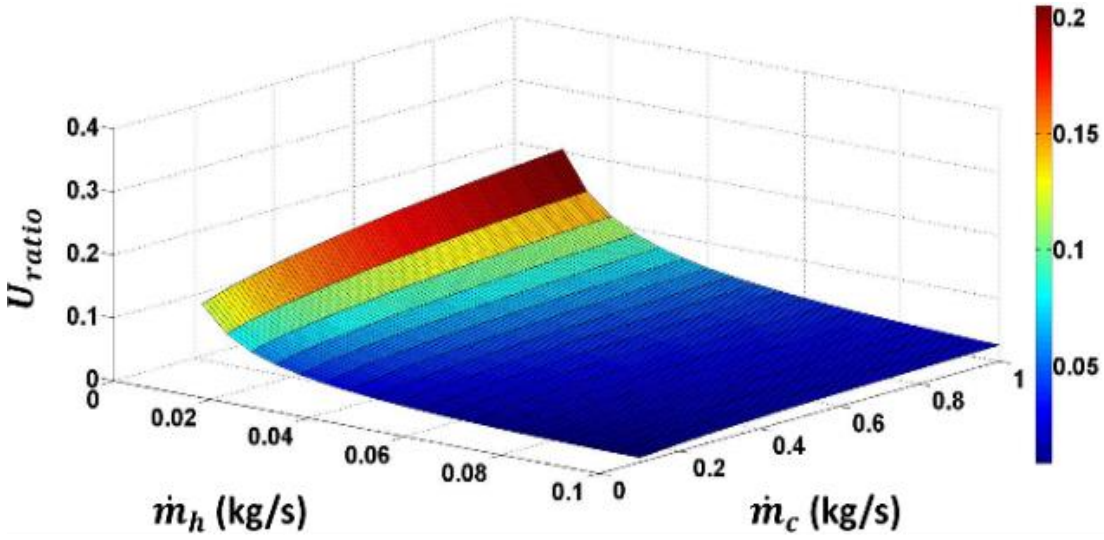

Figure 3-25 : U_{ratio} vs $\dot{m}_h$ vs $\dot{m}_c$ for geometry 4 when pressure drop and compactness are prioritized

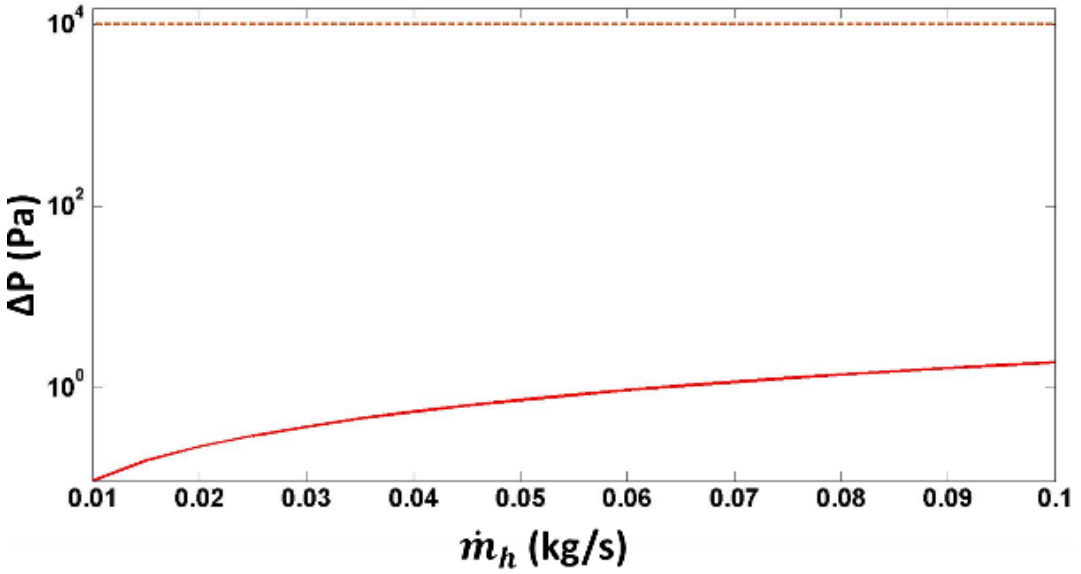

Figure 3-26 : ΔP vs $\dot{m}_h$ for geometry 4 when pressure drop and compactness are prioritized

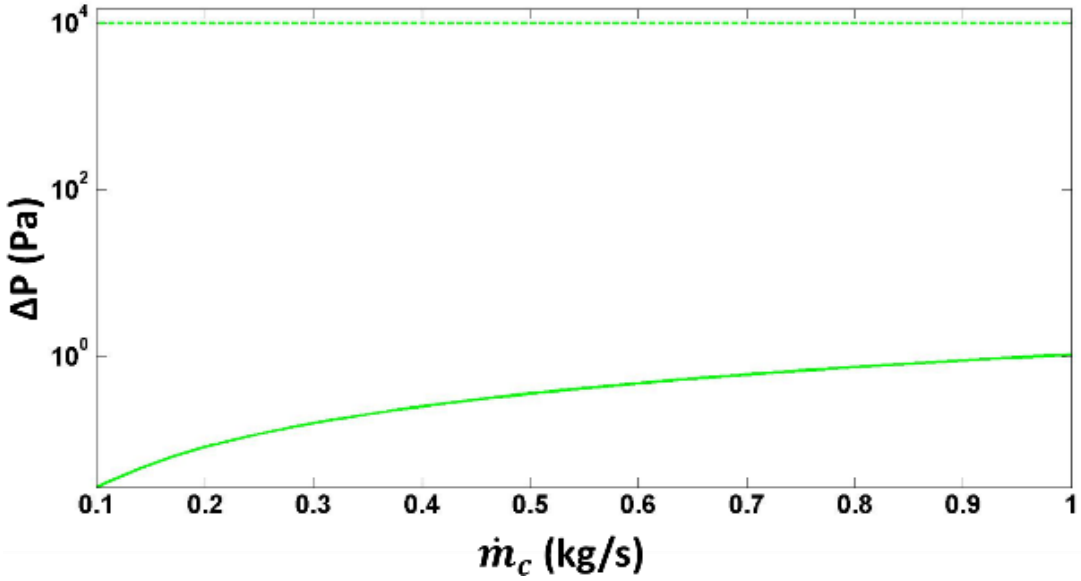

Figure 3-27 : ΔP vs $\dot{m}_c$ for geometry 4 when pressure drop and compactness are prioritized

3.8.3. Heat Transfer and Pressure Drop Prioritized

This section presents design and performance when heat transfer and pressure drop are prioritized. The design parameters for heat exchanger geometries are shown in table 3-11. Figure 3-28 and 3-31 illustrates change in U_{ratio} for different mass flow rate combinations for the given mass flow rate range. U_{ratio} is greater than or equal to 1 in the entire mass flow rate change. For cases where U_{ratio} is lesser than 1, mass flow rate of the hot fluid should be decreased or that of the cold fluid must be increases to bring U_{ratio} to 1.

Table 3-11 : Optimized design parameters when heat transfer and pressure drop are prioritized

Geometry	Length (m)	Diameter (m)	Fin and wall thickness (m)	Channel height (m)		Number of fins		Number of turns	
				Inner	Outer	Inner	Outer	Inner	Outer
5	0.15	0.15	0.002	0.002	0.009	8	8	1.5	1.5
6	0.40	0.25	0.002	0.004	0.012	3	3	0.5	0.5

Increasing or decreasing mass flow rates to satisfy heat transfer goals means going outside the mass flow rate range. For example, in geometry 6 the mass flow rate of the hot fluid must be decreased to 0.0032 kg/s if the hot fluid flows at 0.1 kg/s to achieve U_{ratio} = 1. Figure 3-29, 3-30, 3-32 and 3-33 summarizes the pressure drop for geometries 5 and 6 and are within the threshold for the given mass flow rate range. However, the geometries are not classified as compact since the surface area density/ compactness are less than 400 m2/m3. The volume for design 5 and 6 are 0.0026 and 0.0196 m3 and the mass are 3.64 and 20.73 kg.

To summarize a tradeoff between heat exchange, pressure loss and compactness is observed while designing an optimized model for given set of geometry constraints. To choose a design which takes less space and is lower in weight we have to trade either heat exchange or pressure loss.

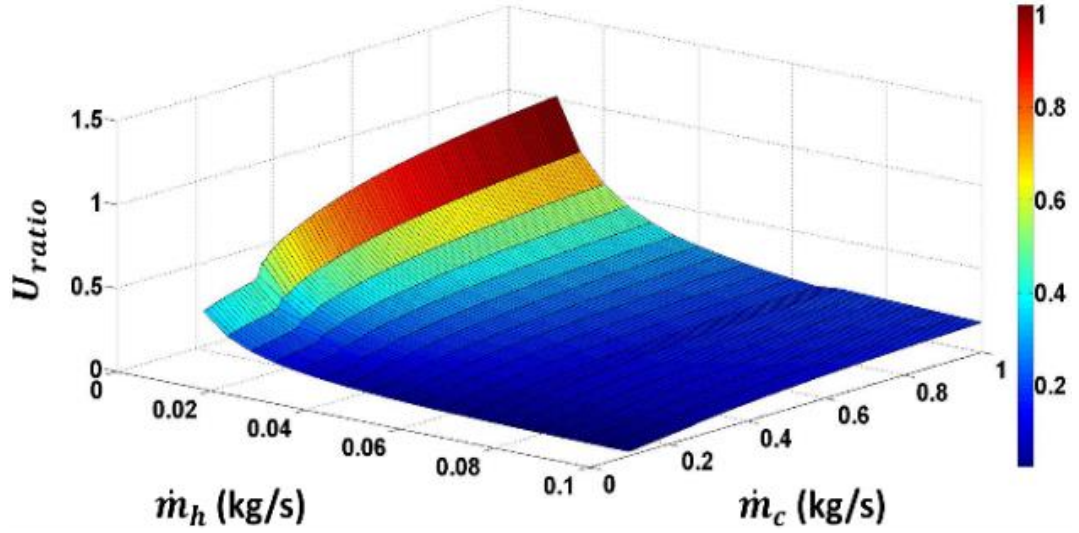

Figure 3-28 : U_{ratio} vs $\dot{m}_h$ vs $\dot{m}_c$ for geometry 5 when heat transfer and pressure drop are prioritized

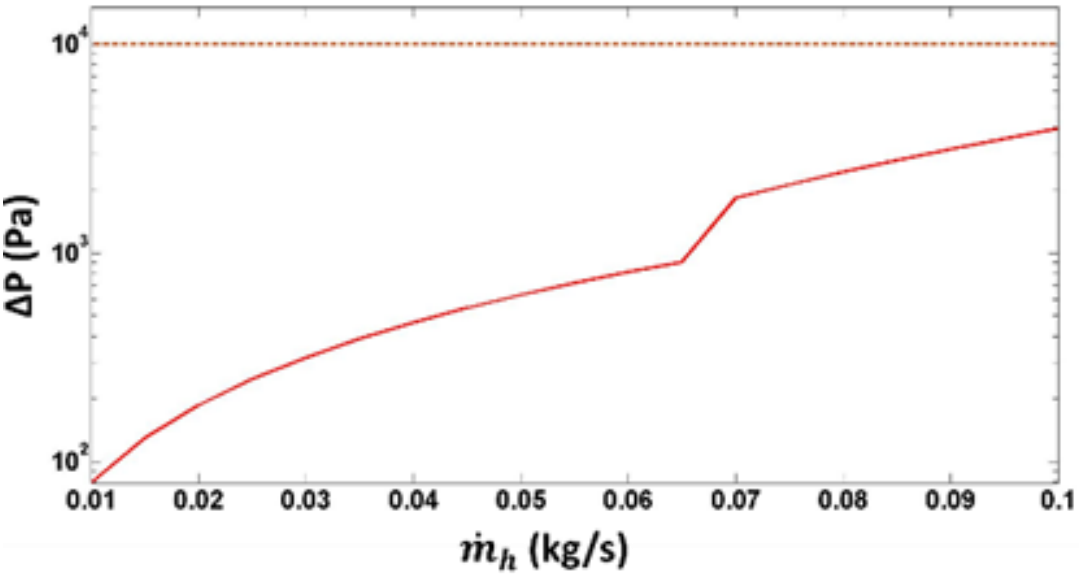

Figure 3-29 : ΔP vs $\dot{m}_h$ for geometry 5 when heat transfer and pressure drop are prioritized

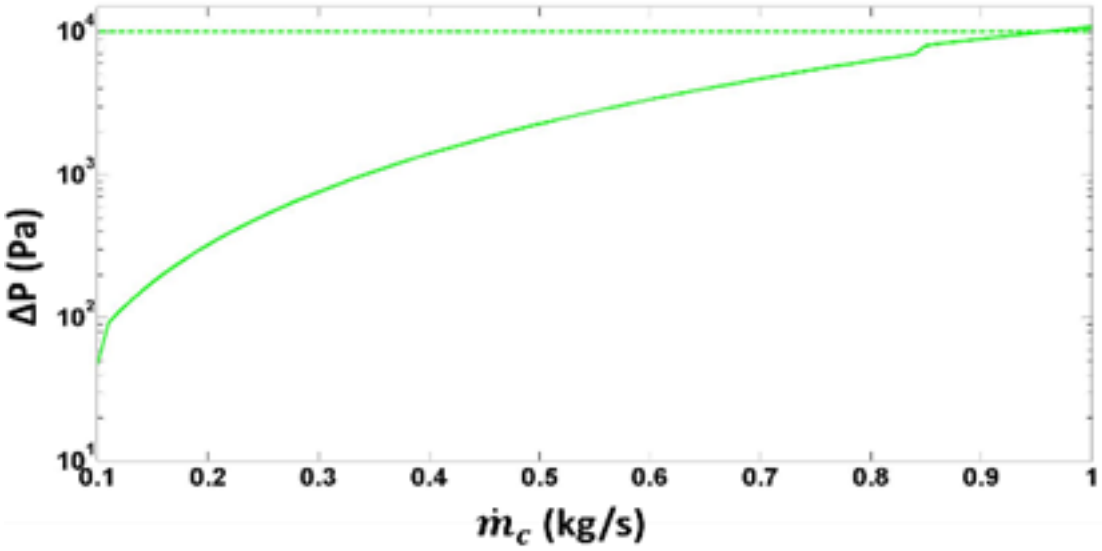

Figure 3-30 : ΔP vs ṁc for geometry 5 when heat transfer and pressure drop are prioritized

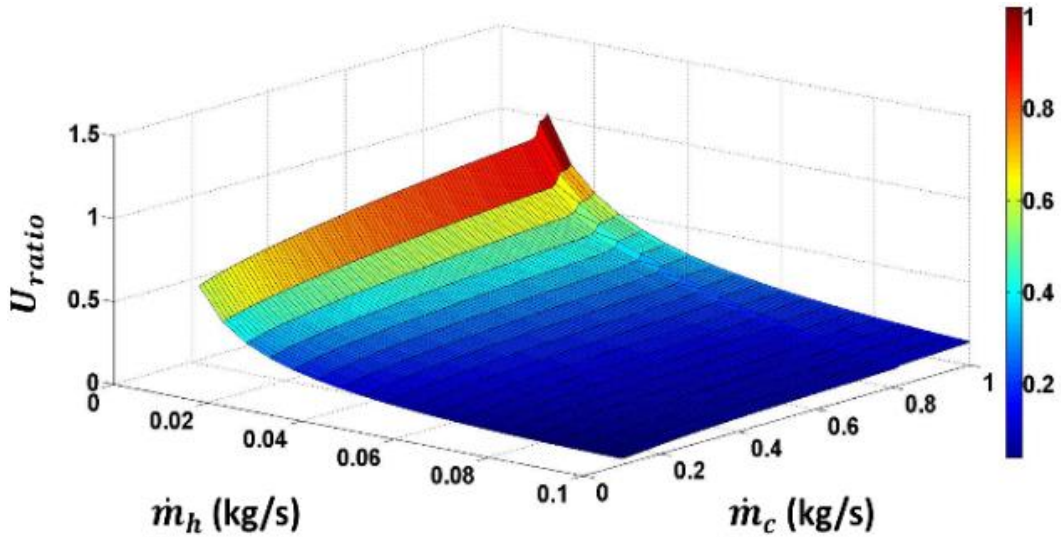

Figure 3-31 : Uratio vs ṁh vs ṁc for geometry 6 when heat transfer and pressure drop are prioritized

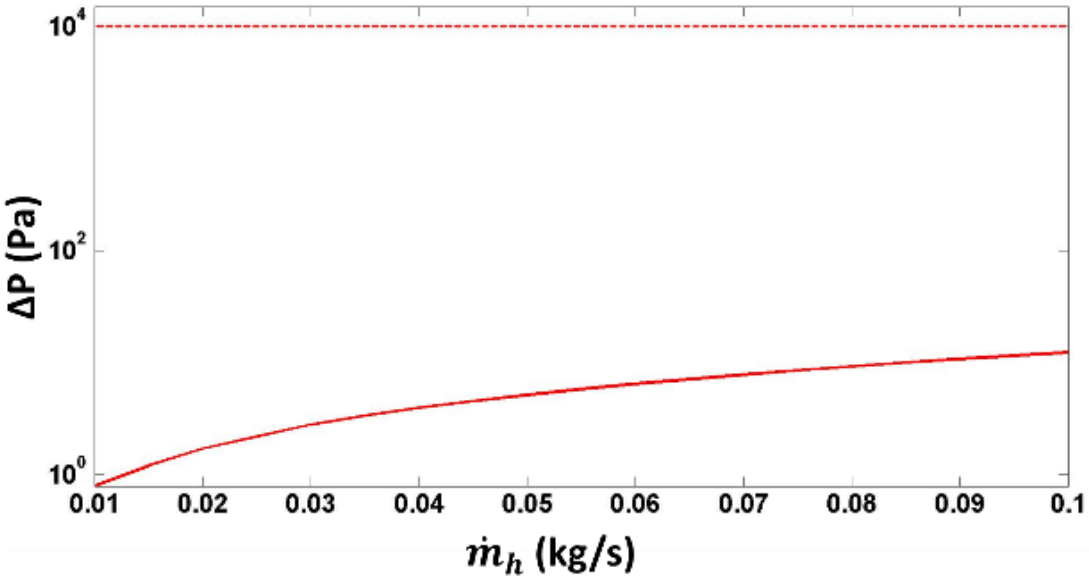

Figure 3-32 : ΔP vs $\dot{m}_h$ for geometry 6 when heat transfer and pressure drop are prioritized

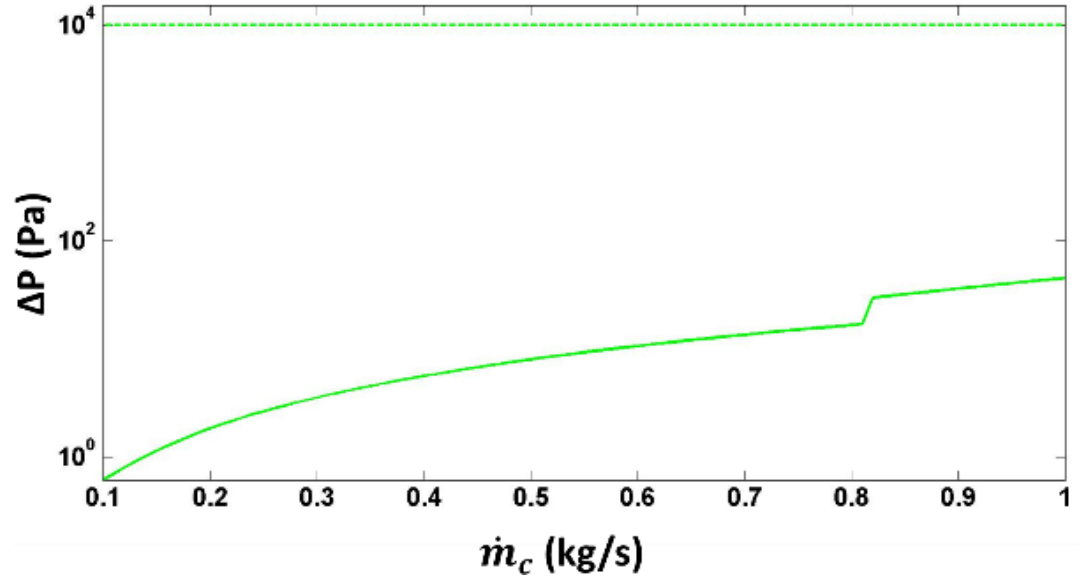

Figure 3-33 : ΔP vs $\dot{m}_c$ for geometry 6 when heat transfer and pressure drop are prioritized

4. Numerical Modeling of Helical Heat Exchanger

4.1. Overview of Numerical Analysis

In this current study, the numerical simulations are conducted in annular heat exchanger with straight radial fins and three helical fin heat exchanger geometry, prioritized for heat and compactness, pressure drop and compactness, heat transfer and pressure drop. Cold and hot water are used as working fluids of the counter flow heat exchanger. The numerical results for the helical fin heat exchanger and straight annular heat exchanger are compared with one dimensional analytical results. Comparison between the analytical and numerical results are made for the heat exchanger performance parameters such as pressure drop and outlet temperatures of the working fluids. The geometry considered for the numerical analysis are shown below in table 4-1. All the cases are performed for a fixed mass flow rate combination of 0.01 kg/s and 1 kg/s for hot and cold fluid respectively. The assumptions for the numerical analysis are made as same as analytical model. Since the innermost and outer walls are insulated – means that no heat transfer, those walls are neglected in three-dimensional model to reduce the computational time.

The 3D model for the numerical analysis are generated using the CATIA and the numerical simulations are performed in ANSYS Fluent. Considering an allowance of the complex design geometry, limitation of the processor speed and inadequacy of the RAM, Finite Volume Method (FVM) is used to solve the partial differential equations of this current study and this method has been widely used in all industrial applications and research.

In order to compare the results of heat exchanger performance between the straight and helical fin, the helical length of the case 2 was considered as a length of the straight annular heat exchanger. Hydraulic diameter of the straight annular heat exchanger is same as the helical fin heat exchanger.

Table 4-1 : Geometry parameters for CFD cases

Geometry parameters	Case 1	Case 2	Case3	Case 4
	Straight annular heat exchanger	**Heat transfer and pressure drop prioritized**	**Pressure drop and compactness prioritized**	**Heat transfer and compactness prioritized**
Length (m)	0.54	0.4	0.15	0.25
Diameter (m)	0.25	0.25	0.15	0.25
Fin and Wall thickness (m)	0.002	0.002	0.001	0.001
Inner channel height (m)	0.004	0.004	0.022	0.015
Outer Channel height (m)	0.012	0.012	0.022	0.020
Number of fins at inner channel	3	3	8	6
Number of fins at outer channel	3	3	2	6
Number of turns at inner channel	-	0.5	2.5	4
Number of turns at outer channel	-	0.5	0.5	4

4.2. Numerical Analysis

Computational Fluid Dynamics using commercial codes of numerical algorithms used to solve the fluid flow problems. It is solving the basic equations of fluid flow and heat transfer by applying the numerical techniques. ANSYS software includes well validated physical modeling capabilities to solve diverse types of real time problems such as fluid flow, electromagnetic problems, heat exchanger, structural analysis, vibration analysis etc. The main advantage of the CFD is reduce time and cost reduction in innovative designs. ANSYS FLUENT package has been used to solve the current heat transfer and fluid flow problem in this dissertation. The most crucial step involved in numerical analysis is that selecting the numerical method to solve the partial differential equation of the specific problem. There are three conventional methods are used in computational analysis to obtain the numerical solution of PDE's (partial differential equations).

1. Finite Difference Method (FDM)
2. Finite Element Method (FEM)
3. Finite Volume Method (FVM)

ANSYS Fluent using Finite Volume Method (FVM) to solve the physical problem. In FVM the domain is discretized into a finite set of control volumes. General conservation equations of mass, momentum, energy etc. are solved in each control volume. Partial differential equations are discretized into a system of algebraic equations then solved numerically to render the solution field. The solved discretized form equation will be used to write a solution algorithm for every iterative process until it satisfies the convergence criteria and stability. In Fluent, the control volumes are corresponding directly with the mesh, means that they are all cell centered. The flow chart in Figure 4-1 is showing the numerical simulation algorithm.

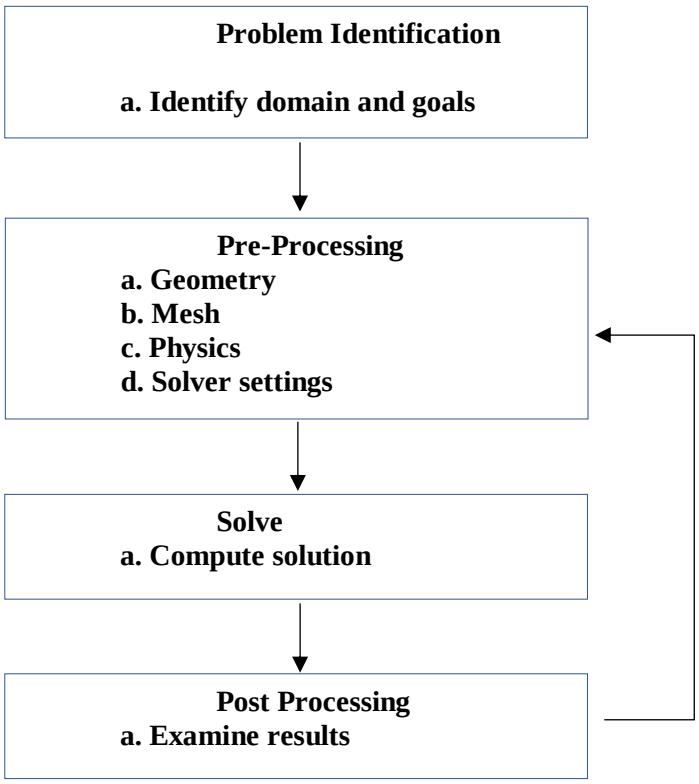

Figure 4-1 : ANSYS Fluent flow chart

4.3. Selection of Turbulence Model and Governing Equations

The accuracy of numerical analysis results are based on the selection of the suitable turbulence model. The selection of the model is depending on the level of accuracy required for the problem, the flow complexity, type of the problem, availability of the computational resources and the simulation time. The available turbulence models in FLUENT are Spalart Allmaras one equation model, and tow equation models such as Standard k- ϵ, RNG k-ϵ, Realizable k-ϵ, Standard k- ω, SST K- ω, detached eddy simulation, large eddy simulation. Each model has its own advantage and disadvantages. Lingdi Tang, Et al **[7]** choose four different turbulence model such as standard k-ϵ model, re-normalization group (RNG) k-ϵ model, SST k- ω model, standard k – ω model to investigate the characteristic of flow in a helical pipe and stated that SST k-ω model was the closest to the experimental test data. Piazza Et al, also showed that SST k- ω model was better in prediction of flow characteristic in helical pipe as compared to standard k-e model. Hence, the SST turbulence model was used for this current study. The governing equations of the SST k- ω model is shown below.

The SST k- ω model (Shear stress transport k- ω) is a variant of the Standard k- ω model. It performs much better than k-ϵ models for boundary layer flows under adverse pressure gradient and separated flows. The governing equations to find kinematic eddy viscosity, turbulence kinetic energy and specific dissipation rate in SST k- ω model is shown bellow.

The turbulent kinetic energy equation is given below in equation (27),

$$\frac{\partial(k)}{\partial t} + U_j \frac{\partial(k)}{\partial x_j} = P_k - \beta * k\omega + \frac{\partial}{\partial x_j}\left[(v + \sigma_\omega v_T)\frac{\partial(k)}{\partial x_j}\right] \tag{27}$$

Where the v_T is kinematic eddy viscosity and given in equation 28,

$$v_T = \frac{a_1 k}{max(a_1\omega, SF_2)} \tag{28}$$

The Specific dissipation rate is given by equation 29 ,

$$\frac{\partial(\omega)}{\partial t} + U_j \frac{\partial(\omega)}{\partial x_i} = \alpha s^2 - \beta\omega^2 + \frac{\partial}{\partial x_j}\left[(v + \sigma_\omega v_T)\frac{\partial(\omega)}{\partial x_j}\right] + 2(1 - F_1)\,\sigma\,\omega^2\,\frac{1}{\omega}\,\frac{\partial k}{\partial x_j}\,\frac{\partial \omega}{\partial x_i} \tag{29}$$

The coefficients and auxiliary relations are given in equations 30, 31,32 and 33.

$$F_2 = tanh\,[\,[\,max\,(\frac{2\sqrt{k}}{\beta * \omega y}, \frac{500v}{y^2\omega} \tag{30}$$

$$P_k = min\,(\tau_{ij}\frac{\partial U_i}{\partial x_j}, 10\beta * k\omega) \tag{31}$$

$$F_1 = tanh\left\{\left\{min\left[max\left(\frac{\sqrt{k}}{\beta * \omega y}, \frac{500v}{y^2\,\omega}\right), \frac{4\sigma_{\omega 2}k}{CD_{kw}y^2}\right]\right\}^4\right\} \tag{32}$$

$$CD_{kw} = max\left(2\rho\sigma_{\omega 2}\,\frac{1}{\omega}\,\frac{\partial k}{\partial x_i}\,\frac{\partial \omega}{\partial x_i}, 10^{-10}\right) \tag{33}$$

4.4. Geometry Modelling

In computational analysis, the first step is creating three-dimensional virtual computer model. In this numerical analysis all the solid models were created using the cad software CATIA v5. To obtain the conformal mesh between the solid and fluid domain, the fluid volume was extracted from the solid body and made as a single part using ANSYS Design Modular. The computational domain of the straight and helical fin heat exchangers (solid and fluid volume) are shown below. In Figure 4-2, 4-3, 4-4 and 4-5. red indicates that the hot fluid domain and Green color indicates the solid volume (solid pipe and fins) and blue color denote cold fluid volume of the heat exchanger.

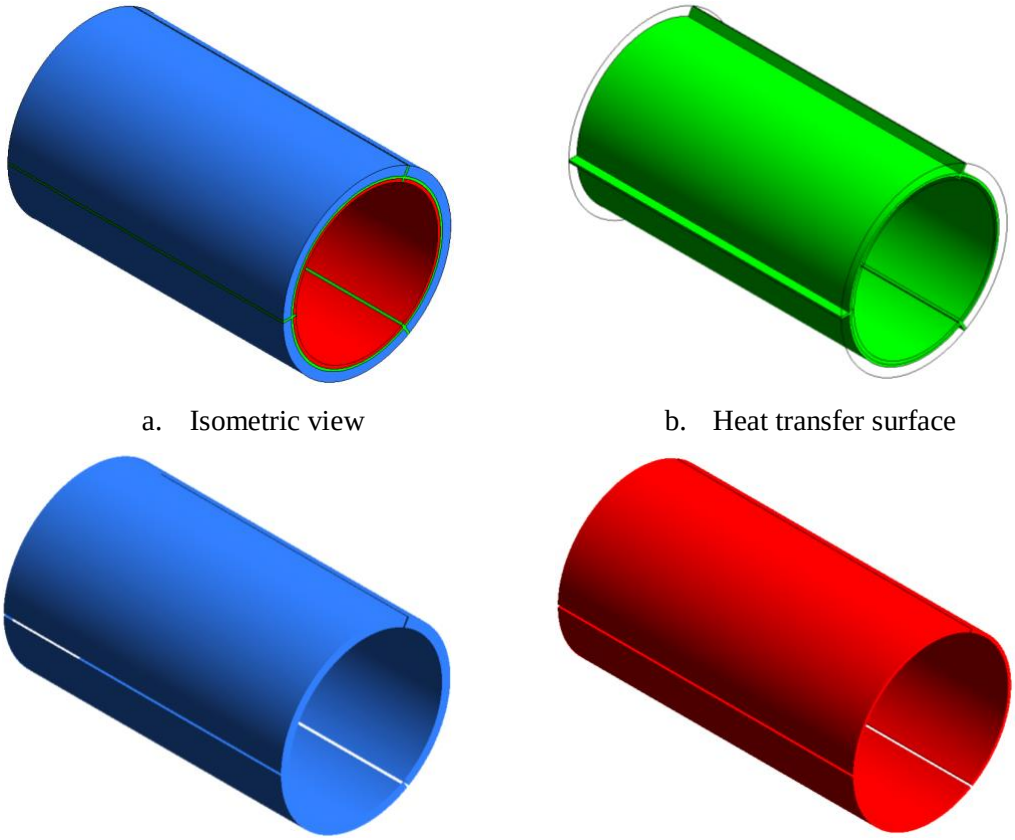

a. Isometric view

b. Heat transfer surface

c. Cold fluid volume

d. Hot fluid volume

Figure 4-2 : Straight annular heat exchanger geometry

In figure 4-2, shown above is the three-dimensional virtual computer model of a straight annular heat exchanger of length 0.541 m, diameter of 0.25 m and fin and wall thickness of 2 mm. Since the outer wall and inner most wall are insulated wall, they are neglected here in the geometry modeling to reduce the computational time as well as reduce the usage of the CPU. It has three straight radial fins parallel to the central axis of the heat exchanger and the flows move parallel to the central axis of the heat exchanger as shown above. The radial elements act as fins to increase the heat transfer area as well as straighten the flow move parallel to central axis.

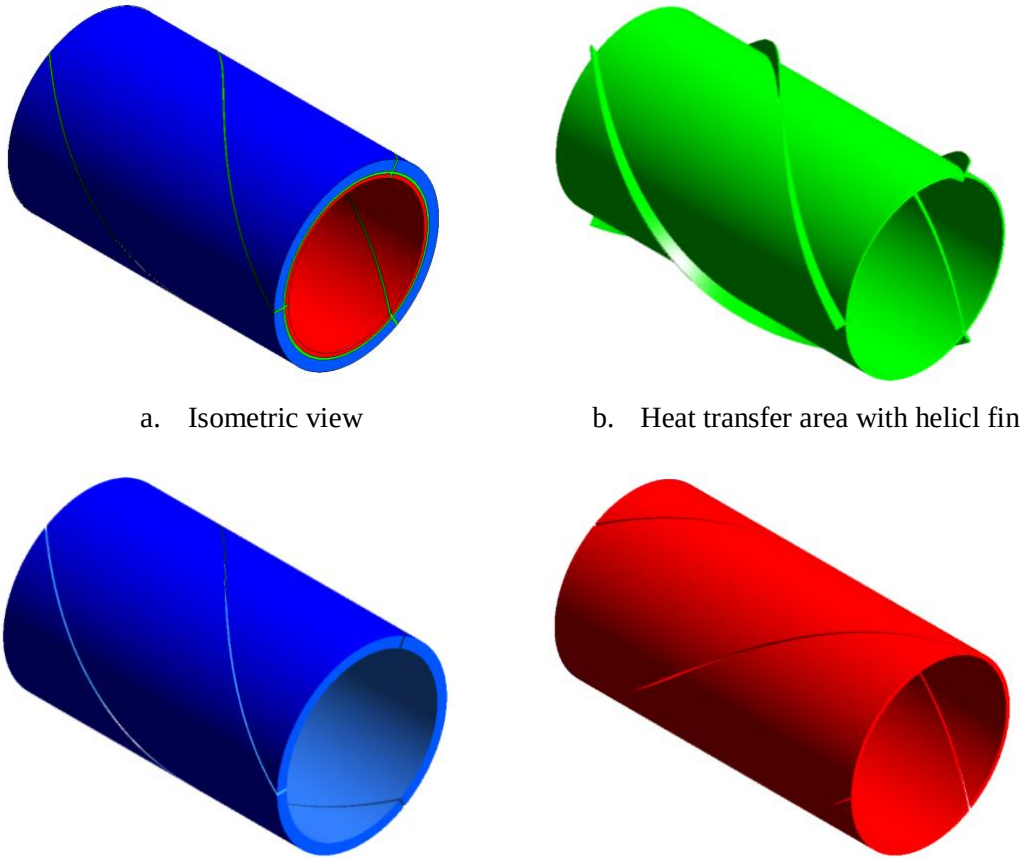

a. Isometric view

b. Heat transfer area with helicl fin

c. Cold fluid volume

d. Hot fluid volume

Figure 4-3 : Heat transfer and pressure drop prioritized geometry

The helical passages are characterized by the number of turns, N, over the length of the heat exchanger, L, or the helical angle Ψ. An isometric view of three-dimensional heat transfer and pressure drop prioritized geometry is shown below in figure 4-4. It has heat exchanger length, L, of 0.4 m, diameter of D, 0.25 m. The three helical fins with 0.5 turns at outer and inner channel which gives helically shaped passages at outer and inner channels respectively. The fin and wall thickness of this model is 2mm. The inner and outer channel heights are denoted by h_i and h_o respectively Ψ represents the helical angle.

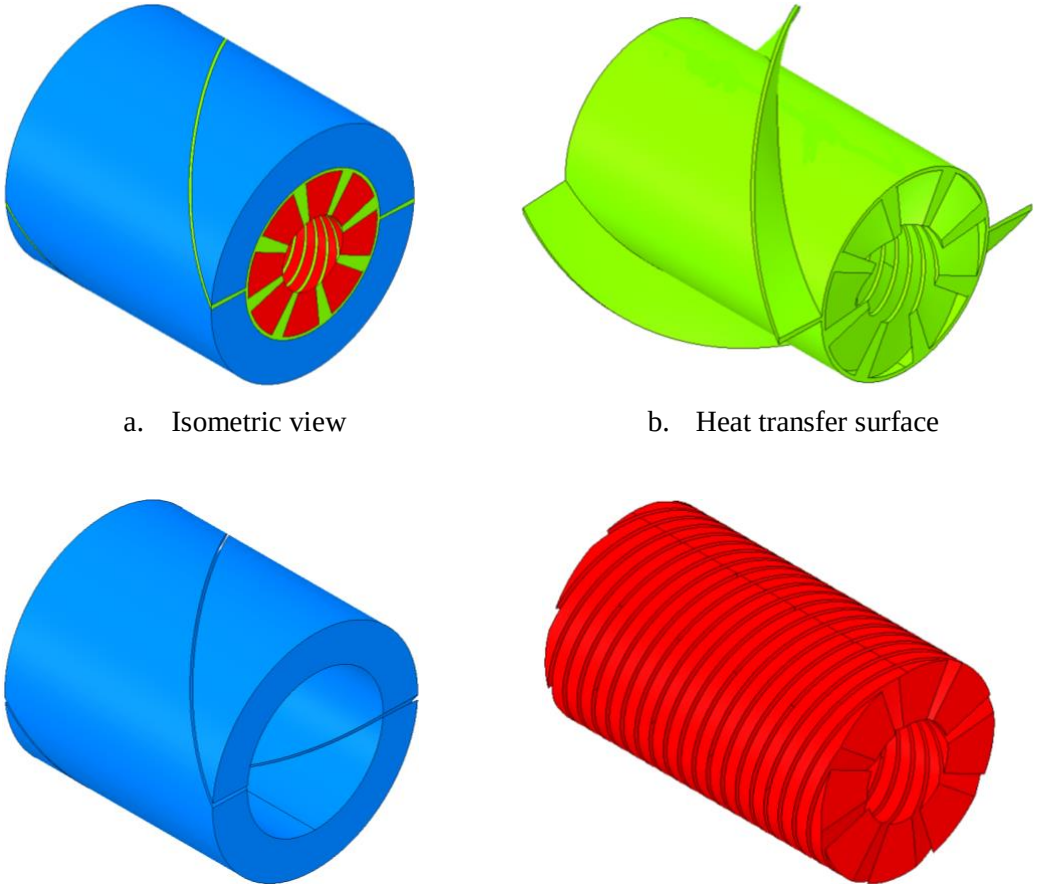

a. Isometric view

b. Heat transfer surface

c. Cold fluid volume

d. Hot fluid volume

Figure 4-4 : Pressure drop and compactness prioritized geometry

The 3D model of the heat pressure and compactness prioritized model is shown above in figure 4-4. The heat exchanger length, L, is 0.15 m and the maximum diameter of the heat exchanger is 0.15 m. It has two helical fins with the thickness of 1 mm and 0.5 turns with no lean angle at outer channel which divide the outer channel into two cold fluid helical passages. There are 8 helical fins with 1 mm of thickness, with no lean angle and 2.5 turns over the length of L at inner channel gives 8 helically shaped passages at hot fluid channel. An isometric view of the 3D model is shown in figure 4-4(a) an the heat transfer surface, cold fluid volume and hot fluid volume are shown in figure 4-4 (b), (c), (d).

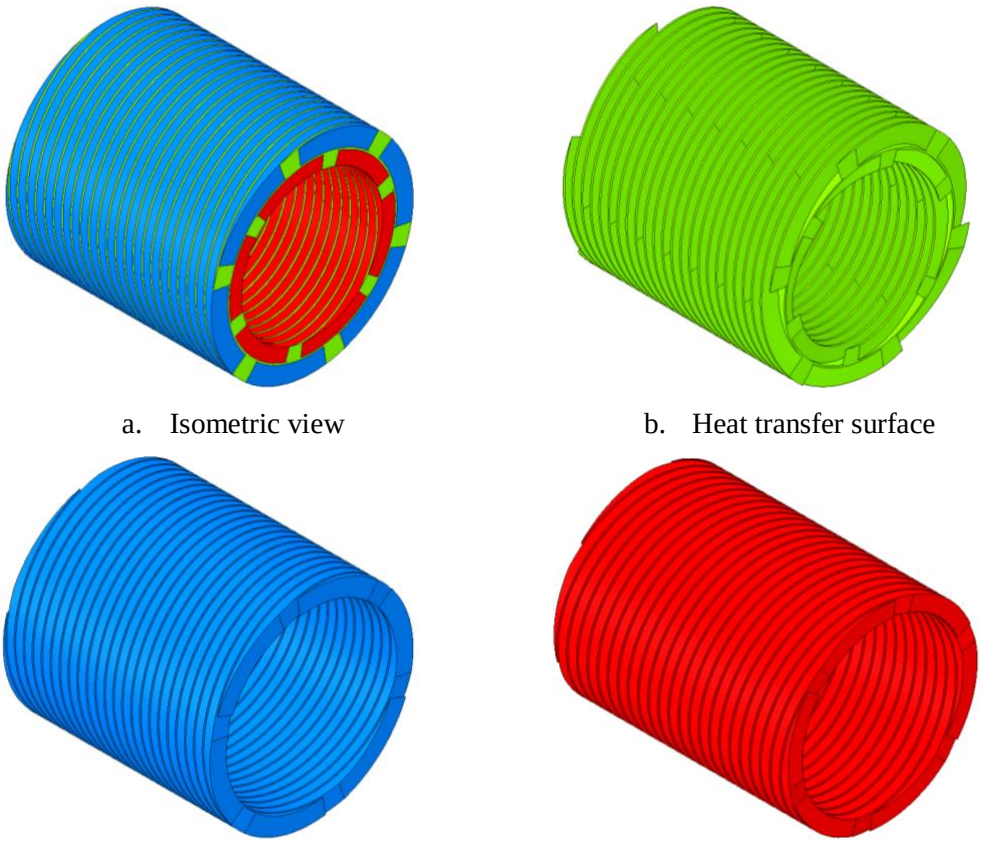

a. Isometric view

b. Heat transfer surface

c. Cold Fluid volume

d. Hot fluid volume

Figure 4-5 : Heat transfer and compactness prioritized geometry

The figure 4-5 shown above is the three-dimensional model of heat transfer and compactness prioritized geometry with the length of 0.25m and maximum diameter of 0.25m. It has 0.015 m inner channel height and 0.020 m of outer channel height. There are 6 helical shaped passages at inner and outer channels divided by 1mm thickness of helical fins with 4 turns over the heat exchanger length of L and no lean angle.

4.5. Meshing

Meshing is an art to discretize the model into small control volumes where the conservative equations of mass and momentum, and energy equations are solved by the numerical method. There are different tools are available such as ICEM CFD, Hyper mesh, ANSYS meshing tool etc., to generate meshing. In this numerical analysis the meshing was generated using Ansys meshing tool. The accuracy of the numerical results is based on the mesh quality and the selection of mesh type. O type mesh, C type mesh, conformal block structured mesh, multiblock structured mesh, non-conformal meshes, unstructured triangular, tetrahedral, quadrilateral, hexahedral and polyhedral meshes are the diverse types of mesh. Type of meshing is very important in numerical analysis which is directly affects the convergence time and numerical results. Some of the 3D cell types are shown below.

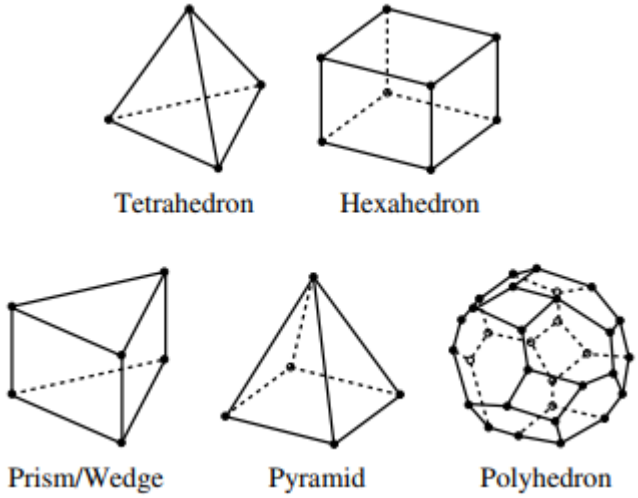

Figure 4-6 : 3D cell types

Hex mesh type is preferred when we require computational efficiency, controlled mesh metrices and have limited computer resources. In this study, hex mesh is used wherever it is possible in this heat exchanger model (mostly on fluid domain) and tetra mesh is used in solid

domain. Though the structured mesh can reduce the computational time and memory usage of the CPU, it is very difficult to obtain the structured mesh throughout the heat exchanger model due to their complex design. However, the conformal mesh was generated to ensure the connectivity between structured and unstructured mesh in fluid and solid domain respectively. The mesh generated for the helical fin heat exchanger is shown below in figure, and the number of elements and nodes on each case are shown in table 4-2.

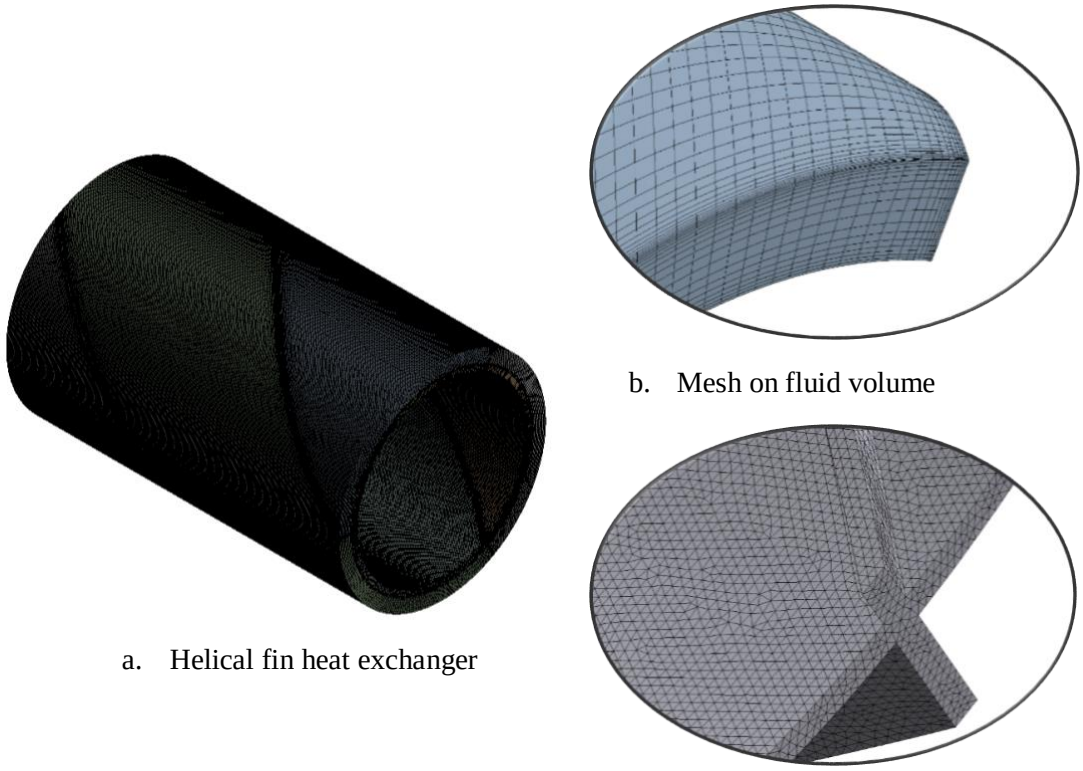

a. Helical fin heat exchanger

b. Mesh on fluid volume

c. Mesh on solid volume

Figure 4-7 : Meshed model of helical fin heat exchanger geometry

To capture the viscous effect and boundary layer separation in flow field, inflation layers (boundary layer) are generated in near wall region of the fluid domain. For the turbulent boundary layers, the boundary layer thickness is calculated using the formula given in equation (34) below,

$$\delta \approx \frac{0.37\,x}{Re_x^{1/5}} \qquad (34)$$

Where Re_x is the Reynolds number, and x is the distance downstream from the start of the boundary layer.

Table 4-2 : Mesh statistics

CFD cases		Cold fluid	Hot fluid	Solid
Straight annular heat exchanger	Nodes	387002	262788	654190
	Elements	347260	216590	484746
Helical fin heat exchanger	Nodes	1246934	431830	1178080
	Elements	1143360	343008	881737

4.5.1. Grid Independence Study

Grid independent study or grid sensitivity study is a most important verification method for any computational study. The numerical results are not only depending on assumptions made, it also depends on the different mesh densities. In this numerical analysis, the grid independent study was carried out by varying the mesh density on cold fluid volume to obtain the pressure loss.

Table 4-3 Grid sensitivity study matrix

Grid #	Number of elements in cold fluid volume	Pressure loss (ΔP) in (Pa)
1	382654	31.3
2	586584	32.8
3	854695	33.7
4	1015246	34.1
5	1143360	34.2

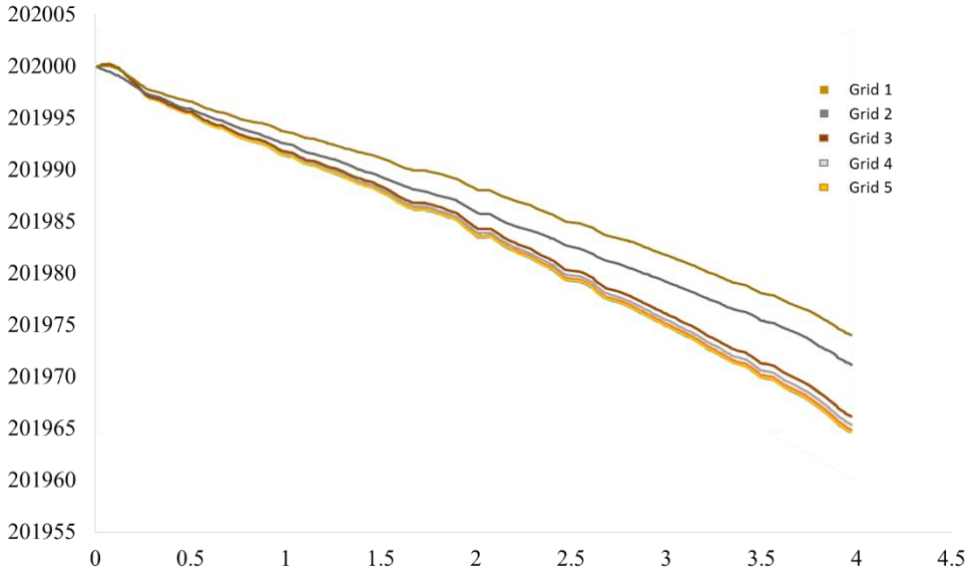

Figure 4-8 : Grid independence study

The ideal grid independent study is to capture accurate physics while keeping the number of cell to minimum to reduce the computational run time. A series of numerical simulation was performed on cold fluid volume from one of the heat exchanger geometry prioritized for U_{ratio} and Compactness. The simulation performed with exact initial and boundary conditions with varying grid spacing i.e. varying grid density.

4.6. Setup of Computational Parameters

The inlet and outlet boundary conditions are given in table 4-4. Boundary condition of cold and hot fluid inlets are mass flow inlet boundaries and it is used to provide a prescribed mass flow rate at the inlet. This inlet boundary condition is often used when a prescribed mass flow rate is important to match of the inflow stream than the total pressure of the inflow. The correct mass flow rate is maintained by adjusting the computed velocity in each iteration. If total mass flow rate is provided at inlet, then FLUENT converts internally to a uniform mass flux by dividing mass flow rate by total inlet area. For incompressible flow, the density of the inlet is either constant or readily computed as the function of temperature and species mass fraction. Pressure outlet boundary conditions were given for the cold and hot fluid channels.

Wall boundary condition of constant heat flux is given for the heat transfer surface i.e. on mid wall, and fins. In geometry modeling the innermost and outermost walls are neglected since they are insulated. A thin surface is considered as a wall with no heat flux condition. The interface between the fluid and solid domain is created using the coupled option in wall thermal boundary condition. The operating pressure of 202 kPa is included in operating boundary conditions.

Table 4-4 : Boundary condition

Parameter	Boundary condition
Cold fluid inlet	Mass flow inlet
Hot fluid inlet	Mass flow inlet
Cold fluid outlet	Pressure outlet
Hot fluid outlet	Pressure Outlet
Mid wall and fins (heat transfer area domain)	Wall boundary, constant heat flux
Fluid and solid interface	Coupled wall

The following assumptions also made for the numerical modeling of the current physical problem.

- Steady and incompressible flow
- Thermo-physical properties of cold and hot fluids are temperature dependent

Pressure - velocity coupling is created using SIMPLE scheme algorithm. Momentum equations discretized by second order upwind scheme. First order upwind scheme algorithm was used to solve the turbulent kinetic energy and specific dissipation rate.

5. Analysis of Numerical Results

In this section presents the numerical results of the straight annular heat exchanger and three optimized heat exchanger geometry.

5.1. Straight Annular Heat Exchanger

By keeping the channel length, hydraulic diameter and number of fins constant, the results of straight and helical fin heat exchangers are compared. The geometry considered for the comparison of thermal performance is given in table 5.

Table 5-1 : Results of straight annular heat exchanger

Parameter	Hot fluid outlet temperature (K)	Cold fluid outlet temperature (K)	Cold fluid pressure loss (ΔP)	Hot fluid pressure loss (ΔP)
1-D Analytical	340	279.3	4.2459	0.471
3-D CFD	342	278.9	4.41	0.491
Difference (%)	0.58	0.14	3.89	4.24

The numerical results of straight annular heat exchanger show that maximum deviation of 4.24% in pressure drop and 0.58% in outlet temperatures in comparison with their corresponding analytical results. Straight fin heat exchanger has 30% more volume and mass than helical fin heat exchanger. It has been found that heat transfer rate on straight annular heat exchanger is 53.6% less than the helical fin heat exchanger having the same geometrical and flow parameter. It also noted that the helical fin heat exchanger is compact (volume and mass) than that of straight annular heat exchanger but the pressure drop of helical fin is more than that of straight annular heat exchanger. The numerical and analytical results of straight annular heat exchanger is shown in table 6.

5.2. Heat Transfer and Pressure Drop Prioritized

The absolute pressure contour obtained for mass flow rate of 0.003kg/s and 0.33Kg/s in hot and cold fluid passage respectively. The numerical results show that 18.98% increase in pressure drop at inner passage and 17.62% increase at outer passage when compared to the analytical results. The main reason for this deviation between the numerical and analytical results are the near wall effect and secondary flow effect on pressure drop considered in numerical model by including the boundary layer thickness in grid generation on fluid volume.

Table 5-2 : Results of heat transfer and pressure drop prioritized geometry

Parameter	Hot fluid outlet temperature (K)	Cold fluid outlet temperature (K)	Cold fluid pressure loss (ΔP)	Hot fluid pressure loss (ΔP)
1-D Analytical	298	283	44.31	0.79
3-D CFD	296.2	284.6	52.12	0.94
Difference (%)	0.60	0.56	17.62	18.98

The visualization of the secondary flow at various planes shown above for pressure drop and compactness prioritized geometry. The secondary flow near the wall has been captured by plotting the streamlines at various planes along the heat exchanger length. The flow visualization for the first four planes from the inlet of the geometry has been clearly visible whereas the other planes the magnitude of the secondary flow become smaller. To effectively capture the secondary flow near outlet requires high quality mesh

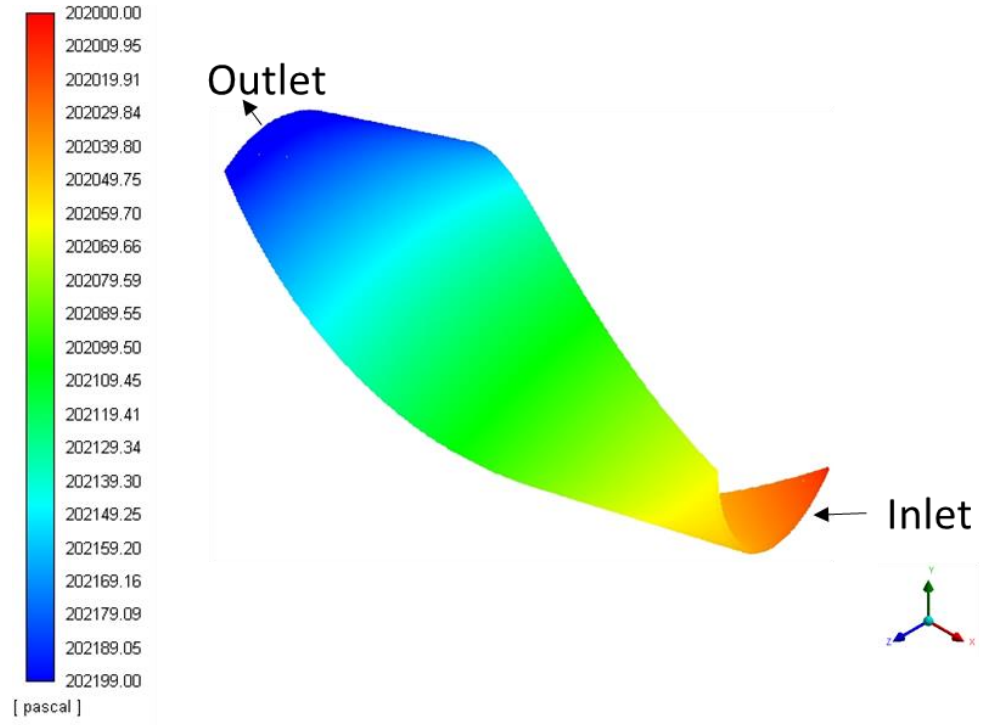

Figure 5-1 : Pressure contour for heat transfer and pressure drop prioritized geometry

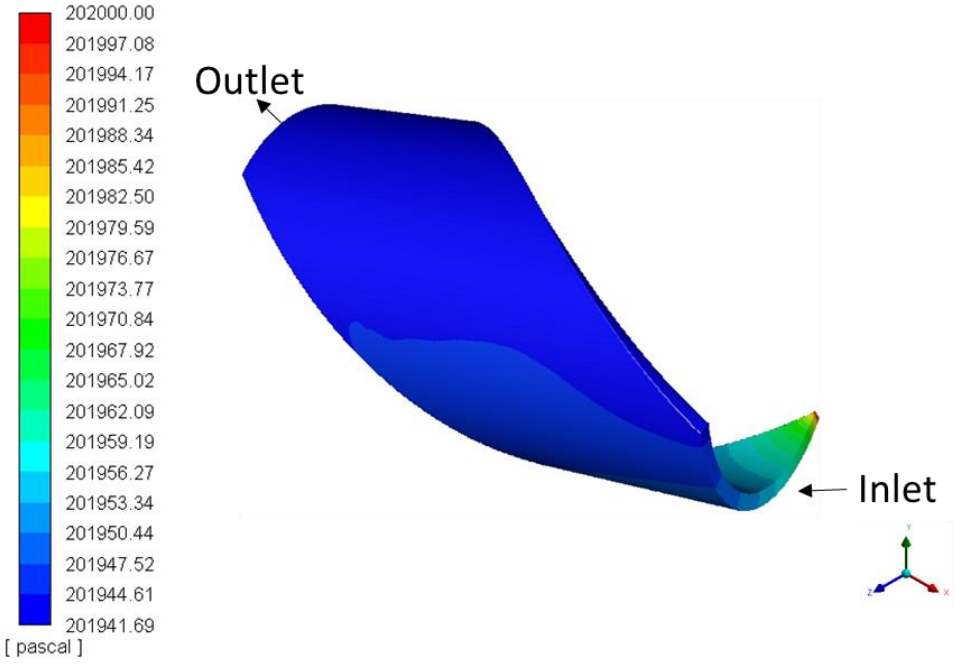

Figure 5-2 : Pressure contour for heat transfer and pressure drop prioritized geometry

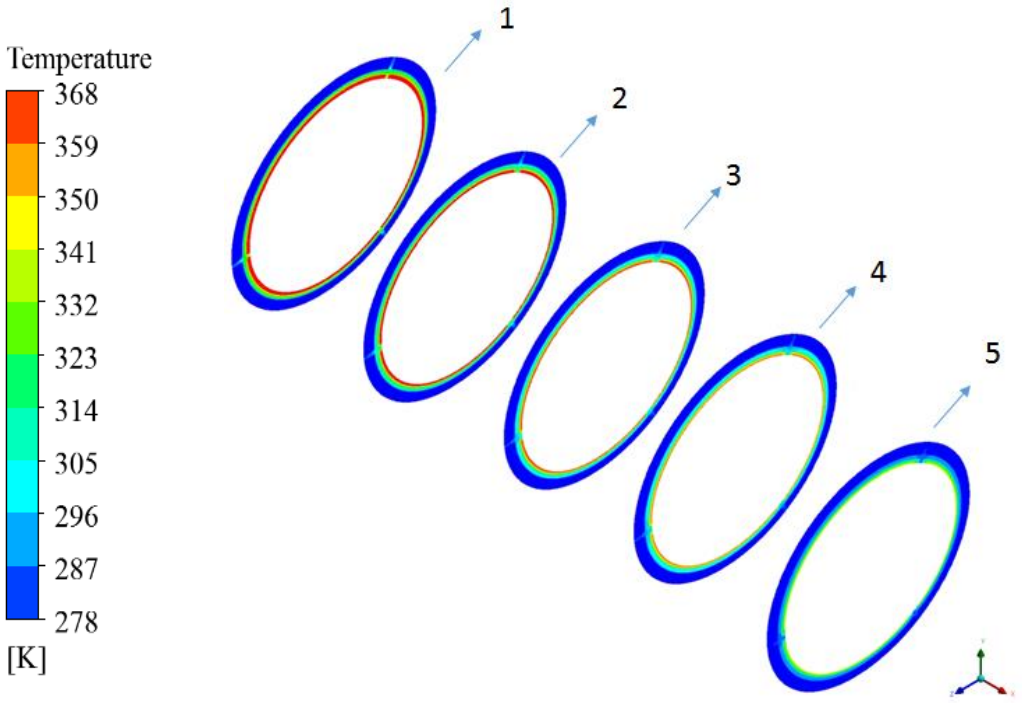

Figure 5-3 : Temperature contour for heat transfer and pressure drop prioritized geometry

Temperature contour has been shown in 5 different planes, equally spaced from hot inlet / Cold outlet to hot outlet / cold inlet. Plane 1 represents hot inlet/ cold outlet whereas plane 5 at hot outlet/ cold inlet. Temperature contour obtained for mass flow rates of 0.01 kg/s and 1 kg/s for hot and cold fluid respectively. Hot fluid has been cooled down from 368 K to296.2 K while cold fluid temperature changes from 278 K to 284.6 K and it has been clearly noted from plane 1 to plane 5. The numerical result shows that the outlet temperature of the hot fluid is cooled down 0.6% more than that the analytical result while cold fluid temperature increases 0.56% more than analytical result.

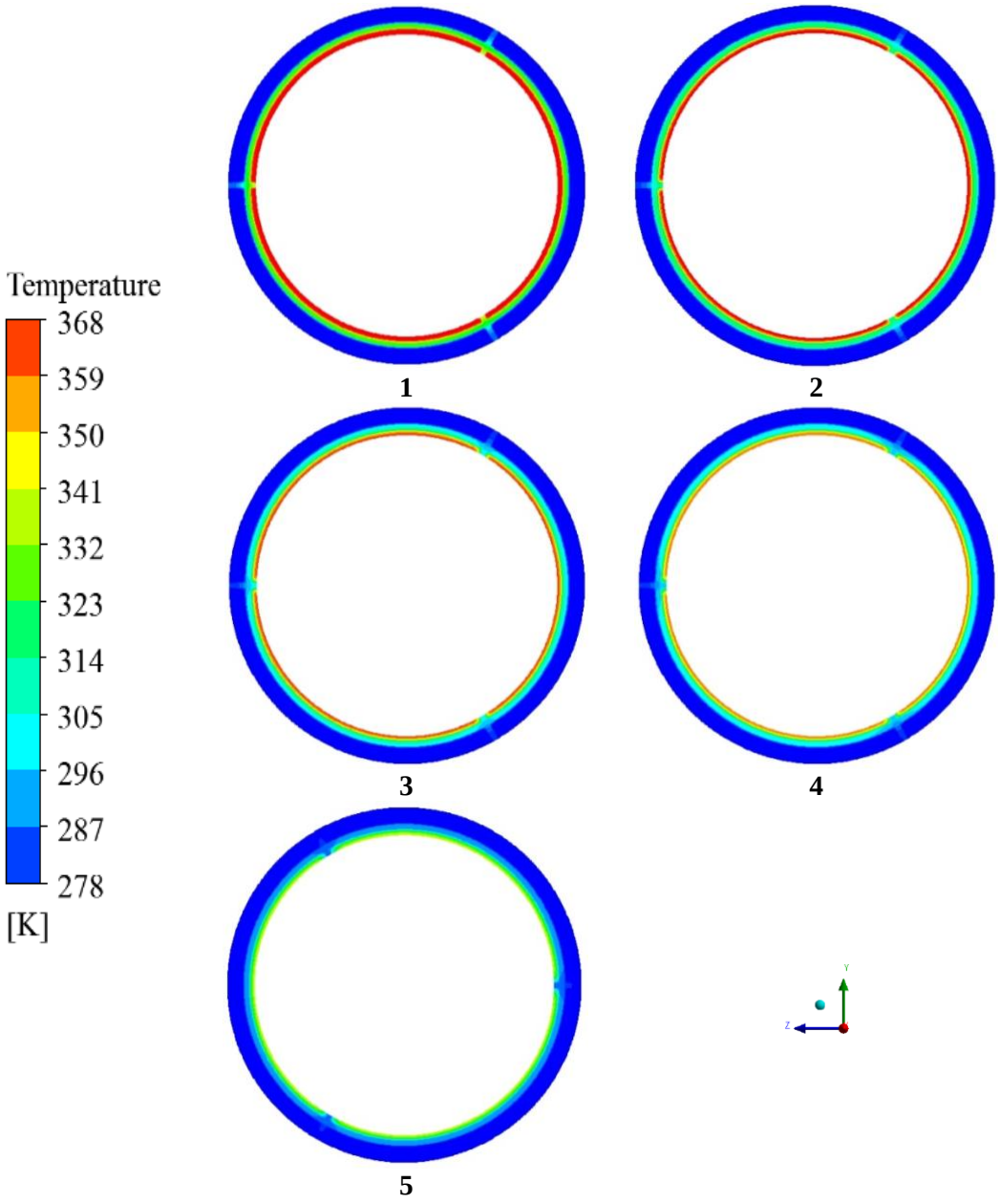

Figure 5-4 : Temperature contour at various planes

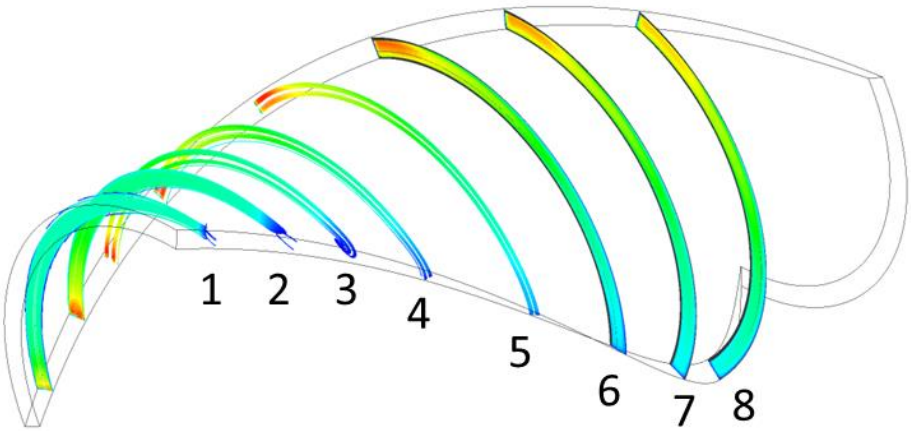

a. Secondary flow at cold fluid channel

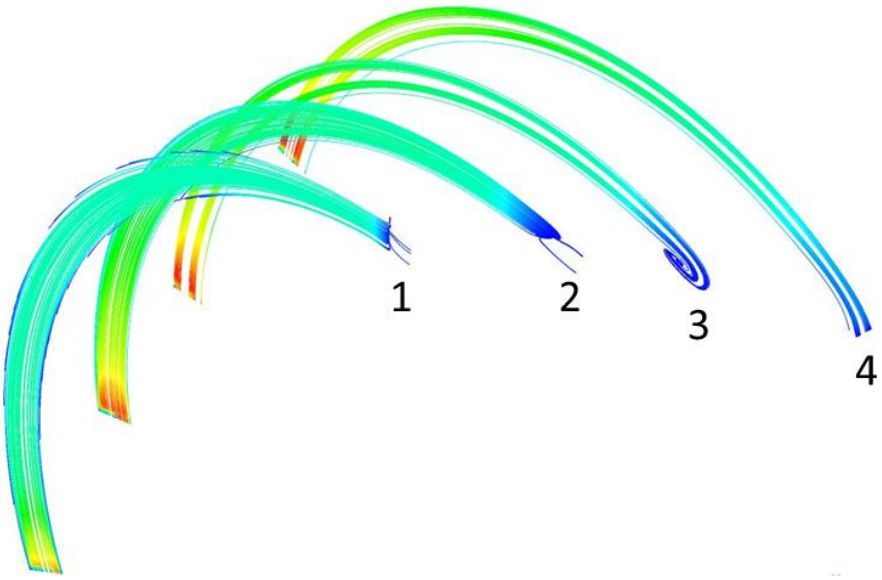

b. Secondary flow viualization at first four planes

Figure 5-5 : Secondary flow visualization of heat transfer and pressure drop prioritized geometry

5.3. Pressure Drop and Compactness Prioritized

Pressure contour for pressure drop and compactness prioritized geometry is obtained for mass flow rates of 0.01kg/s and 1kg/s for hot and cold fluid respectively. The pressure drop of the hot fluid is increases 32% than the analytical result whereas the cold fluid pressure drop increases more 37.15%. When compared heat transfer and pressure drop prioritized geometry, the pressure drop for the current geometry (Pressure drop and heat transfer prioritized) is less.

Table 5-3 : Results of pressure drop and compactness prioritized

Parameter	**Hot fluid outlet temperature (K)**	**Cold fluid outlet temperature (K)**	**Cold fluid pressure loss (ΔP)**	**Hot fluid pressure loss (ΔP)**
1–D Analytical	347	292	24.57	1.449
3-D CFD	338	298	33.70	1.92
Difference (%)	2.59	2.01	37.15	32.5

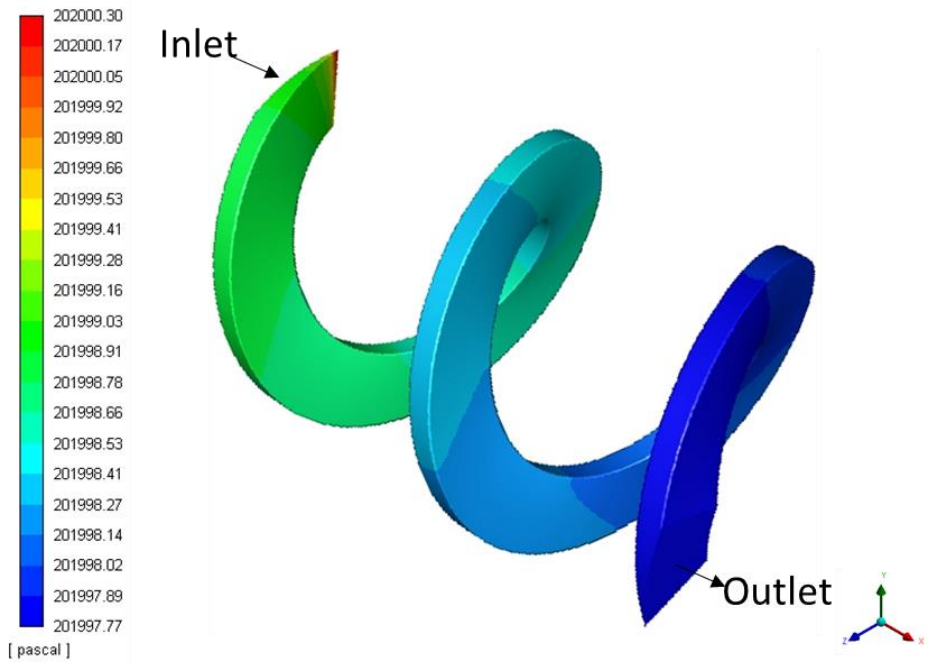

Figure 5-6 : Pressure contour for heat transfer and pressure drop prioritized geometry

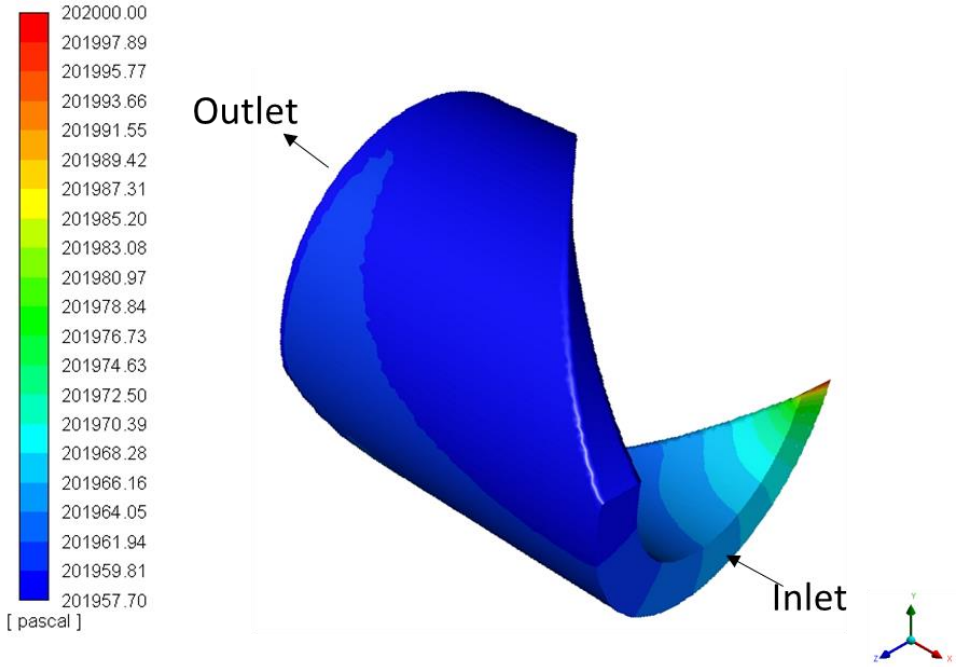

Figure 5-7 : Pressure contour for heat transfer and pressure drop prioritized geometry

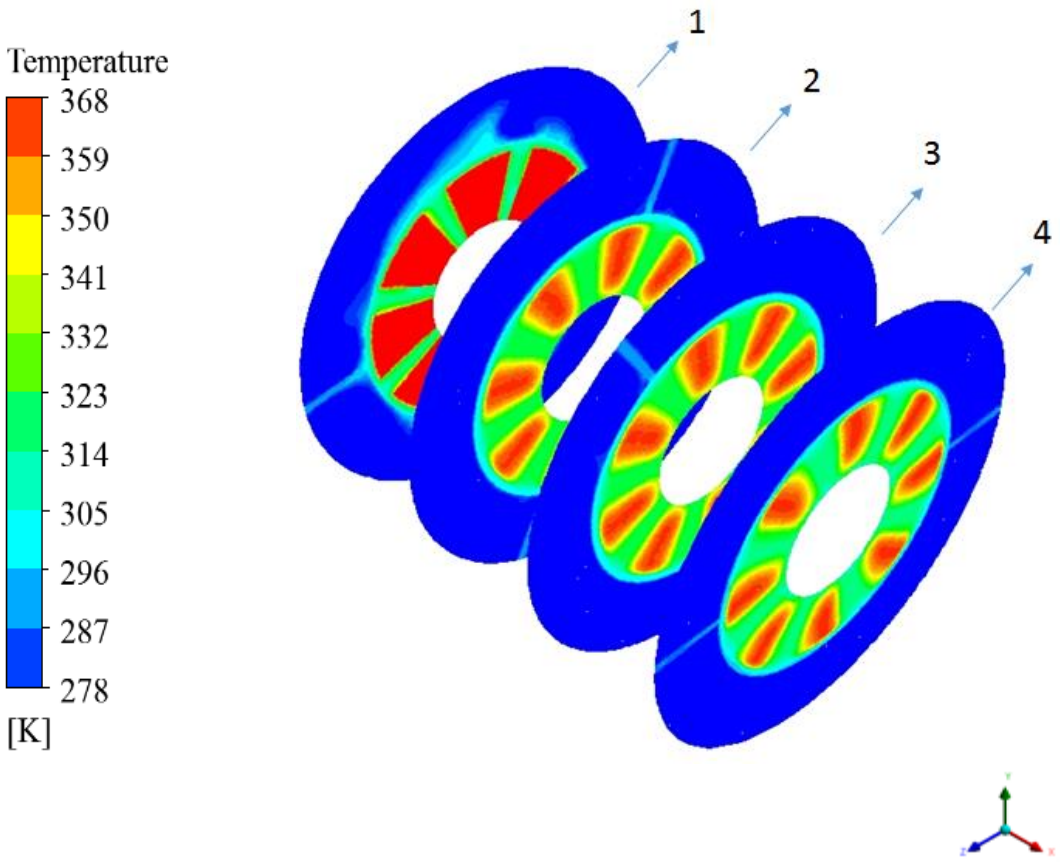

Figure 5-8 : Temperature contour for pressure drop and compactness prioritized geometry

The above temperature contour was obtained for the geometry prioritized for pressure drop and compactness. Since the heat transfer is not prioritized the heat exchange between the fluids is less where as the pressure drop is below the desire range. The hot fluid enters at 368K and cools down to 347K and it can be noted that on plane 1 and 4. The surface integral of the outlet temperature was calculated to find working fluid outlet temperatures

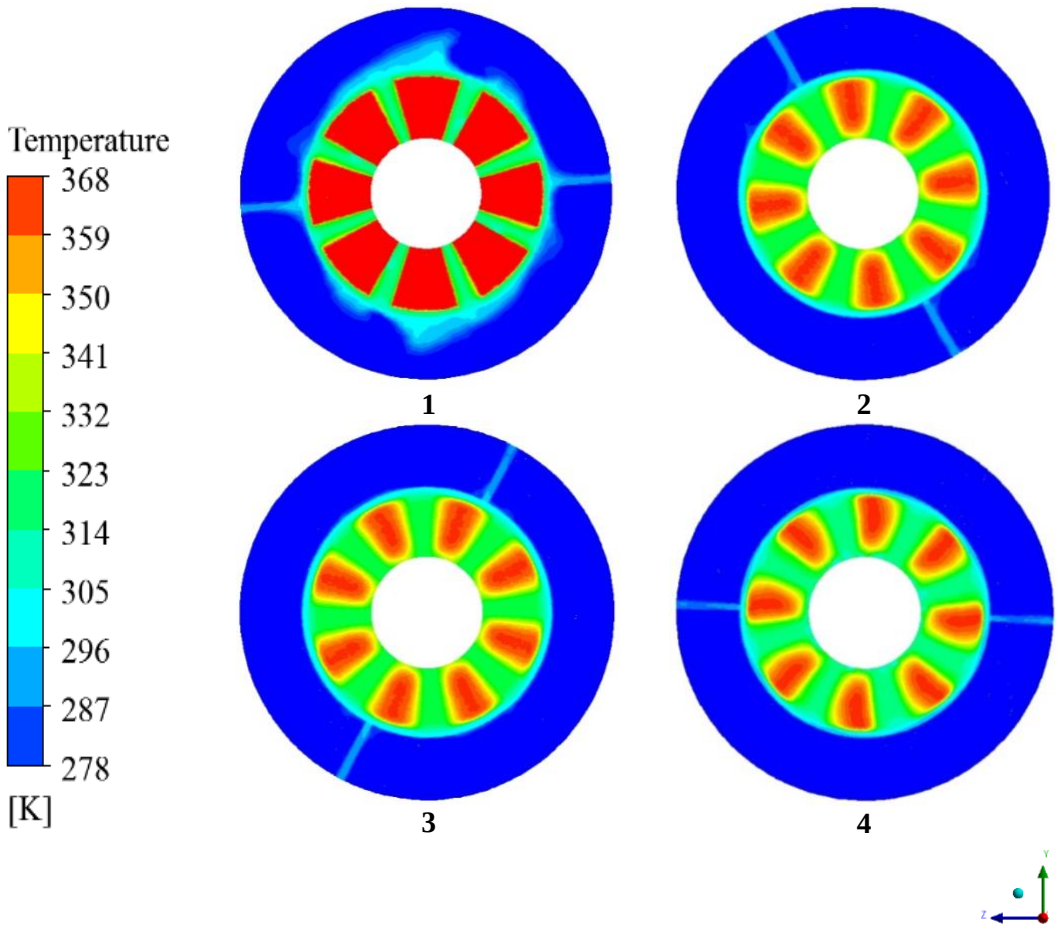

Figure 5-9 : Temperature contour at various planes

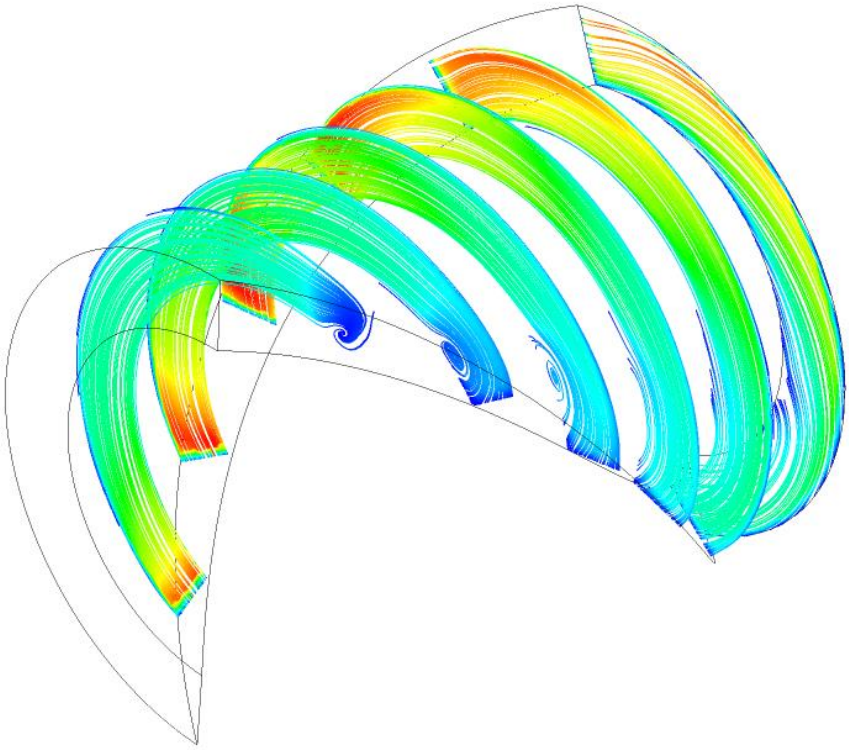

Figure 5-10 : Secondary flow visualization of pressure drop and compactness prioritized geometry

The visualization of secondary flow is illustrated by plotting streamlines at various planes in cold fluid passage of heat transfer and pressure drop prioritized geometry. The figure above shows the evolution of streamlines along the length of the heat exchanger. Velocity magnitude variation has been superimposed on these streamlines. The secondary flow occurs at regions of low velocity (blue regions) magnitude. Flow mixing results in heat transfer enhancement and even temperature distribution near the fins. However, this secondary flow causes more pressure drop across the heat exchanger

5.4. Heat Transfer and Compactness Prioritized

The absolute pressure drop of inner and outer fluid helical passage was observed from inlet to outlet. The pressure contour was obtained for the mass flow rate of 0.01kg/s and 1 kg/s of hot and cold fluid respectively. It has been noted that cold fluid pressure drop increases 32.5% and hot fluid pressure drop increases 36.5% from their analytical results. When number of turns increases the pressure drop also increases.

Table 5-4 : Results of compactness and heat transfer prioritized

Parameter	**Hot fluid Outlet temperature (K)**	**Cold fluid outlet temperature (K)**	**Cold fluid pressure loss (ΔP)**	**Hot fluid pressure loss (ΔP)**
1-D Analytical	299	294	13577.5	5.45
3D CFD	296	298	17998.2	7.44
Difference (%)	1.0	1.36	32.5	36.5

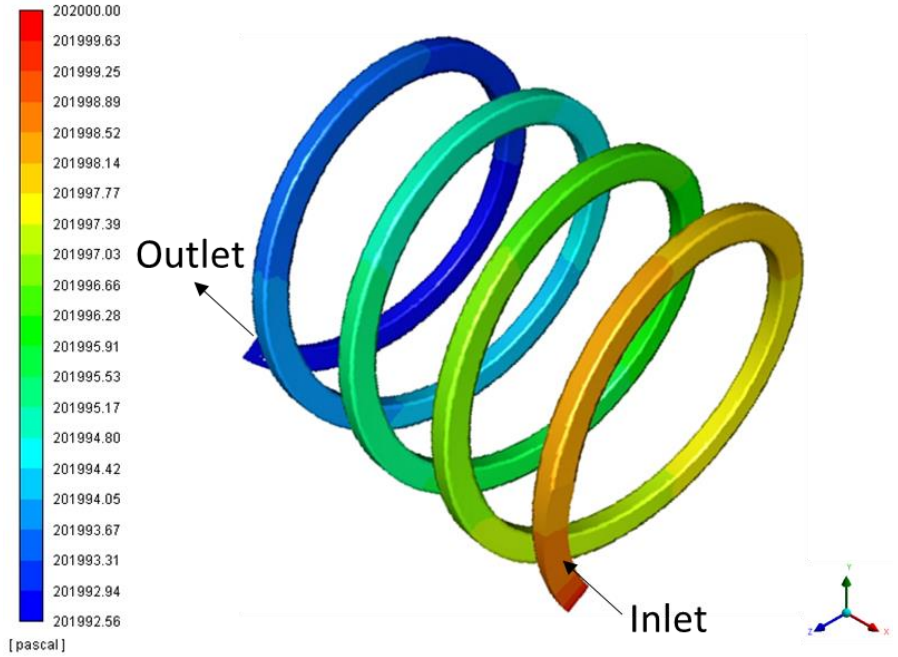

Figure 5-11 : Pressure drop contour for heat transfer and compactness prioritized geometry

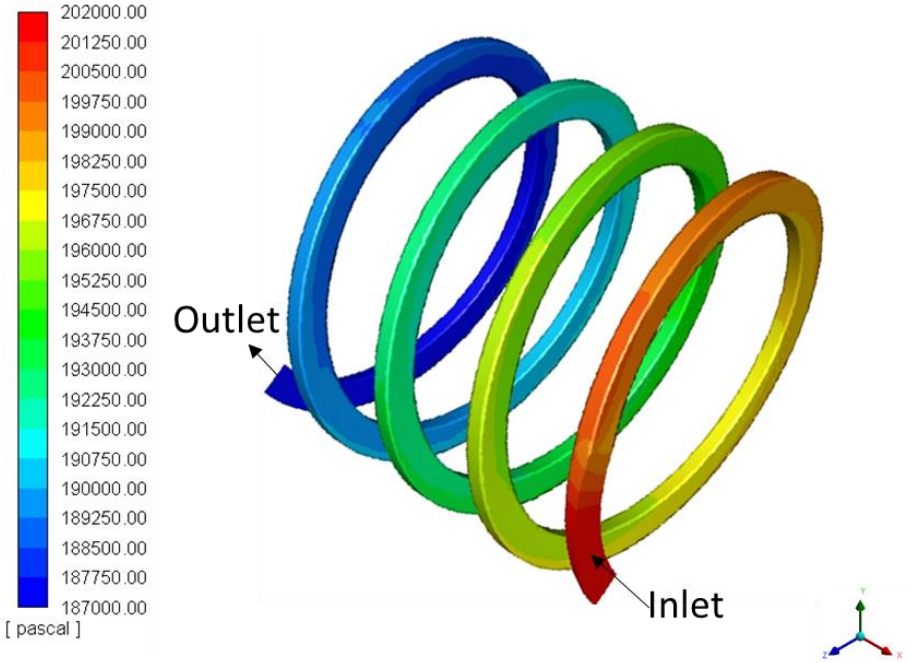

Figure 5-12 : Pressure drop contour for heat transfer and compactness prioritized geometry

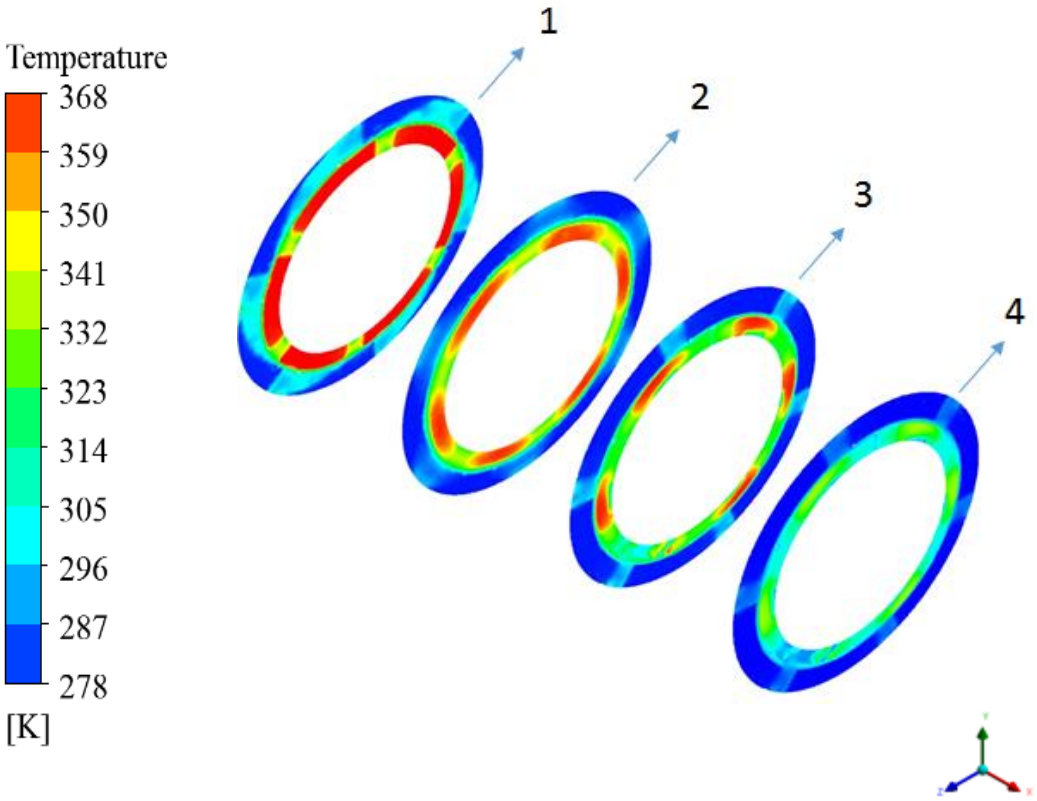

Figure 5-13 : Temperature contour for heat transfer and compactness prioritized geometry

The figure above shows the temperature contour for various planes along the heat exchanger length of 0.25m, inner and outer channel height of 0.015 and 0.020m respectively. The fin and wall thickness of the heat exchanger is 1mm. The hot fluid enters at 368K which is seen by red inner channel in plane 1 and leave at xx K. From plane 4 to plane 1 it's been seen that the temperature of the cold fluid is increases near the fin and wall region due to mixing of fluid by secondary flow generation.

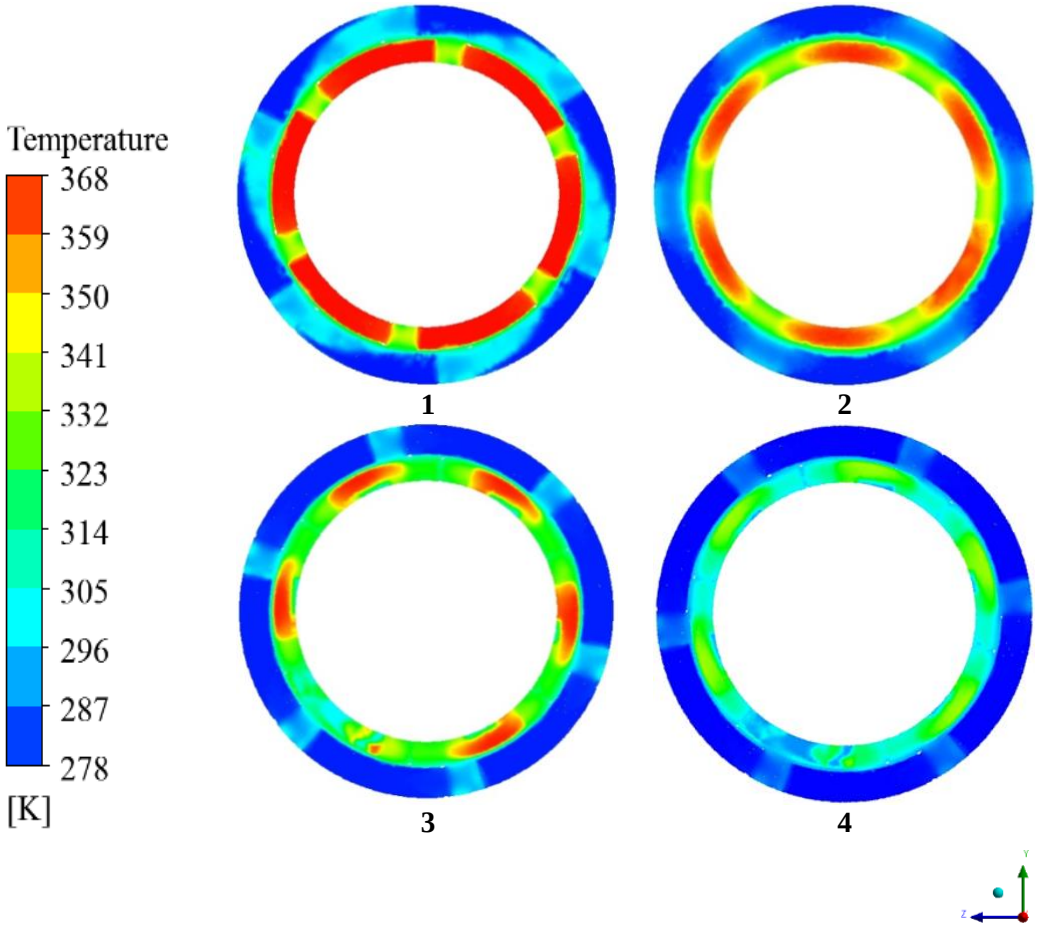

Figure 5-14 Temperature contour at various planes

The vortices (secondary flow) was presented by plotting streamlines at various planes from plane 1 to 3 the vortices start increasing and double vortices start occurring at plane 4. In plane 5 the double vortices of the rectangular cross section is clearly visible and formed symmetrically on the two corners of the cross section of the passage. Its start decreasing after three turns and it can be seen from plane 6,7 and 8, this damping in vortices is caused because of relaminarization effect on the helical pipe

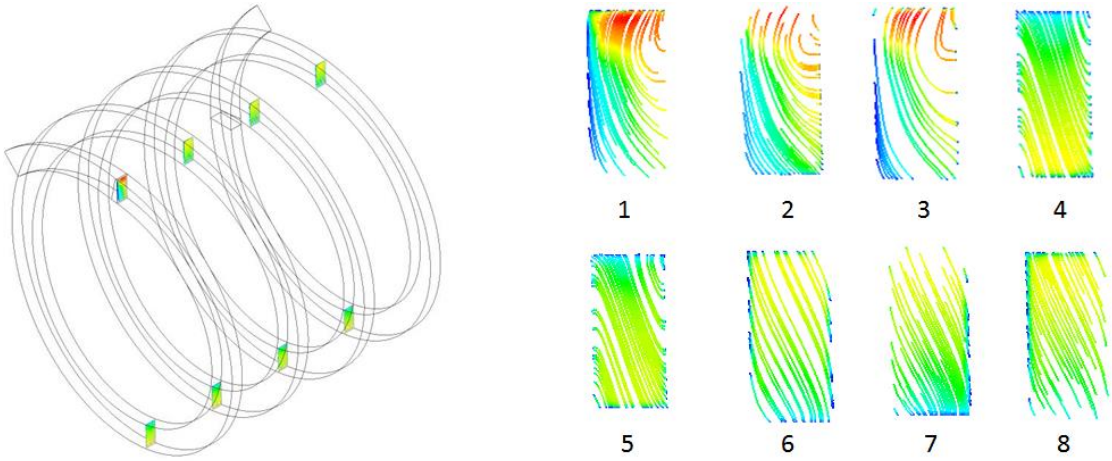

Figure 5-15 : Secondary flow visualization of compactness and heat transfer prioritized geometry

It has been found that the passage diameter affects the secondary flow generation. When the passage diameter is low, the secondary flows are weaker and hence the mixing is lesser. The hydraulic diameter of the helical heat exchangers is shown below in table 5-5.

Table 5-5 : Hydraulic diameter of the cold and hot fluid passage

Helical heat exchanger cases	Hydraulic diameter of cold fluid passage (m)	Hydraulic diameter of hot fluid passage (m)
Pressure drop and compactness prioritized	0.0094	0.027
Heat transfer and pressure drop prioritized	0.0077	0.021
Compactness and heat transfer prioritized	0.0124	0.011

6. Conclusions and Future Work

This work determined the flow characteristics within the helical passage by 3D computational analysis. The numerical results of four different cases with the mass flow rate of 0.01kg/s and 1 kg/s of hot and cold fluid mass flow rates respectively, were calculated and compared with one dimensional analytical model. Finite Volume Method is used to solve conservative equations of mass and momentum and energy equations. SST K-omega model was considered for modeling the turbulence in helical passage heat exchanger.

1-D analytical model can be used as tool to rapidly scope and optimize new heat exchanger designs within a now determined level of accuracy (as compared with a detailed 3D CFD model)

- Maximum outlet temperature and pressure drop difference between 3D CFD 1-D analytical results was determined for several HEX concepts
    - For a straight annular heat exchanger with range of inlet mass flow rates corresponding to 0.01kg/s and 1kg/s for hot and cold fluid respectively, CFD predicted maximum pressure drop difference of +4.24% and outlet temperature is +0.58% as compared with 1-D model
    - For a helical heat exchanger is 27% and outlet temperature is -4.63%.
- By keeping channel length, hydraulic diameter and number of fins constant, results obtained for straight and helical fin heat exchangers are compared.
    - Straight fin heat exchanger has 30% more volume and mass than helical fin heat exchanger
    - However, heat transfer rate is 56% more than straight annular heat exchanger and pressure drop also increases in helical fin heat exchanger.
    - The secondary flow was visualized by illustrating the streamlines on various planes along the heat exchanger length.
    - Compactness of the geometry was determined by calculating the surface area density of the heat exchanger and it was greater than 400 m2/m3.

This concept can be applied in designing heat exchangers for space and automotive applications with different fluids. Future work will include structural analysis and experimental investigations of the proposed compact heat exchanger design.

7. References

[1] Haolin Ma, "Computational Fluid Dynamics and Heat Transfer Analysis for a Novel Heat Exchanger," *Journal of Heat Transfer*, pp. Vol. 137 / 051801-1, 2015.

[2] https://www.additively.com/en/learn-about/3d-printing-technologies.

[3] http://www.materialise.com/en/manufacturing/additive-manufacturing.

[4] J. S. Jayakumar, Helically Coiled Heat Exchangers, Heat Exchangers – Basics Design Applications, 2012.

[5] Y. Z. Y. Li, "Three-Dimensional Numerical Simulation on the Laminar Flow and Heat Transfer in Four Basic Fins of Plate-Fin Heat Exchangers," *Journal of Heat Transfer*, pp. Vol. 130 / 111801-1, 2008.

[6] Samuel D. Marshall, "Heat Exchanger Improvement Via Curved Microfluidic Channels: Impacts of Cross- Sectional Geometry and Dean Vortex Strength," *Journal of Heat Transfer*, pp. Vol. 140 / 011801-1, 2018.

[7] S. P. O. Amir Jokar, "Heat Transfer and Fluid Flow Analysis of Nanofluids in Corrugated Plate Heat Exchangers Using Computational Fluid Dynamics Simulation," *Journal of Thermal Science and Engineering Applications*, pp. Vol. 5 / 011002-1, 2013.

[8] A. B. Withada Jedsadaratanachai, "Performance analysis and flow visualization in a round tube heat exchanger inserted with wavy V-ribs," *Advances in Mechanical Engineering* , p. Vol. 9(9) 1–16, 2017.

[9] W. I. A. Aly, "Computational Fluid Dynamics and Optimization of Flow and Heat Transfer in Coiled Tube-in-Tube Heat Exchangers Under Turbulent Flow Conditions," *Journal of Thermal Science and Engineering Applications*, pp. Vol. 6 / 031001-1, 2014.

[10] L. W. Y. H. Yongheng Zhang, "Study of Heat Transfer Performance of Tube-Fin Heat Exchanger with Interrupted Annular Groove Fin," *IEEE*, pp. 978-1-61284-459-6/11, 2011.

[11] G. M. CHANG Zhen1, "Numerical Simulation and Analysis for the U-tube Heat Exchanger of Ground Source Heat Pump," in *Proceedings of the 32nd Chinese Control Conference* , China, 2013.

[12] K. Thulukkanam, Heat exchanger Design Handbook, CRC PressTaylor & Francis Group, 2013.

[13] Gobetz, "Utiliza tion o f Additive Manufacturing for Aerospace Heat Exchangers," Applied Research Laboratory, State College, PA 16804, 2016.

[14] https://www.nasa.gov/exploration/systems/sls/nasa-tests-3-d-printed-rocket-part-to-reduce-future-sls-engine-costs.

[15] R. M. a. S. W. Churchil, "Fully developed laminar convection from a helical coil," *Chem. Eng. Commun*, vol. 9, pp. 185 - 200, 1981.

[16] G. R. T.J. Rennie, "Numerical studies of a double-pipe helical heat exchanger," *Applied Thermal Engineering*, vol. 26, pp. 1266-1273, 2006.

[17] J.S. Jayakumara, "Experimental and CFD estimation of heat transfer in hellically coiled heat exchangers," *Cehmical Engineering Res. Des*, vol. 86, pp. 221-232, 2008.

[18] R. Manglik, "Heat transfer enhancement," in *Heat Transfer Handbook*, NJ, Wiley: Hoboken, 2003, p. Ch 14.

[19] C. D. M. a. K. K. Harris, "Design and Fabrication of a Cross Flow Micro heat exchanger," *Journal of Microelectro- mechanical Systems,* vol. 4, no. 9, pp. 502-508, 2009.

8. Appendix: Thermophysical properties of working fluids

1) Water

Density vs Temperature

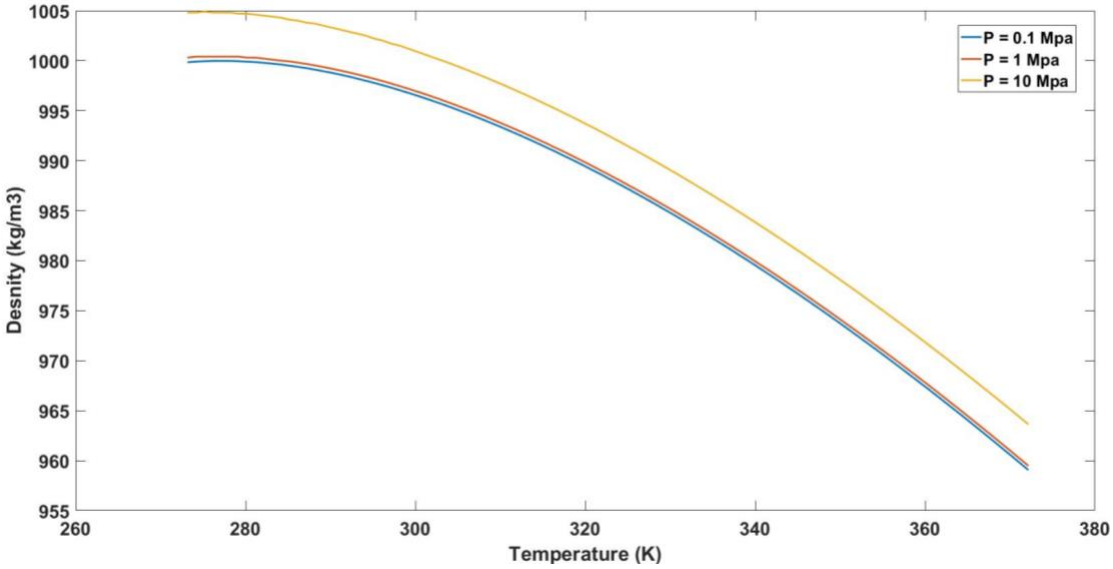

Specific heat at constant pressure vs Temperature

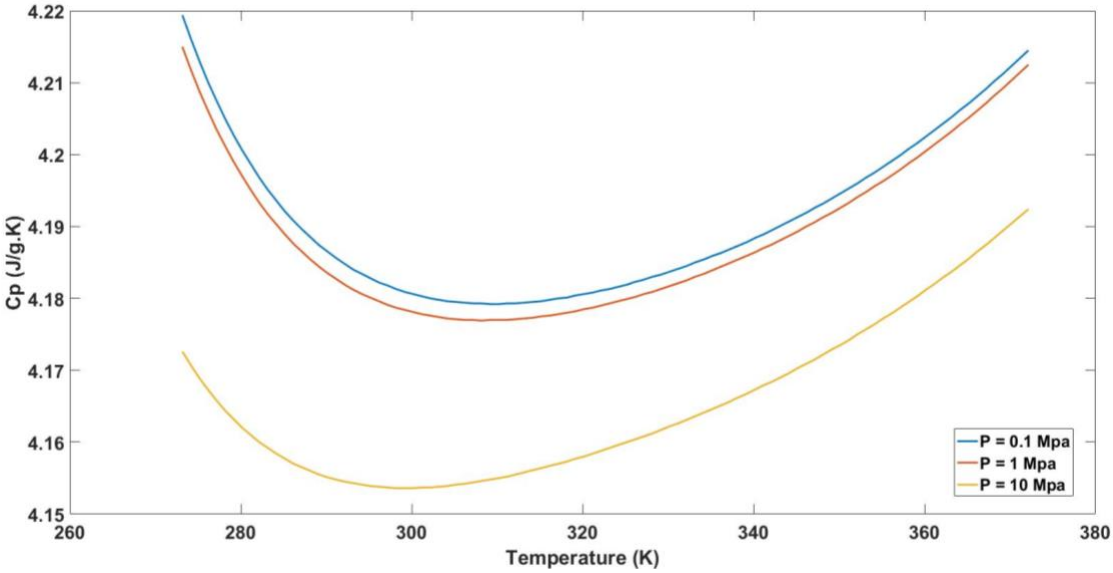

Thermal conductivity vs Temperature

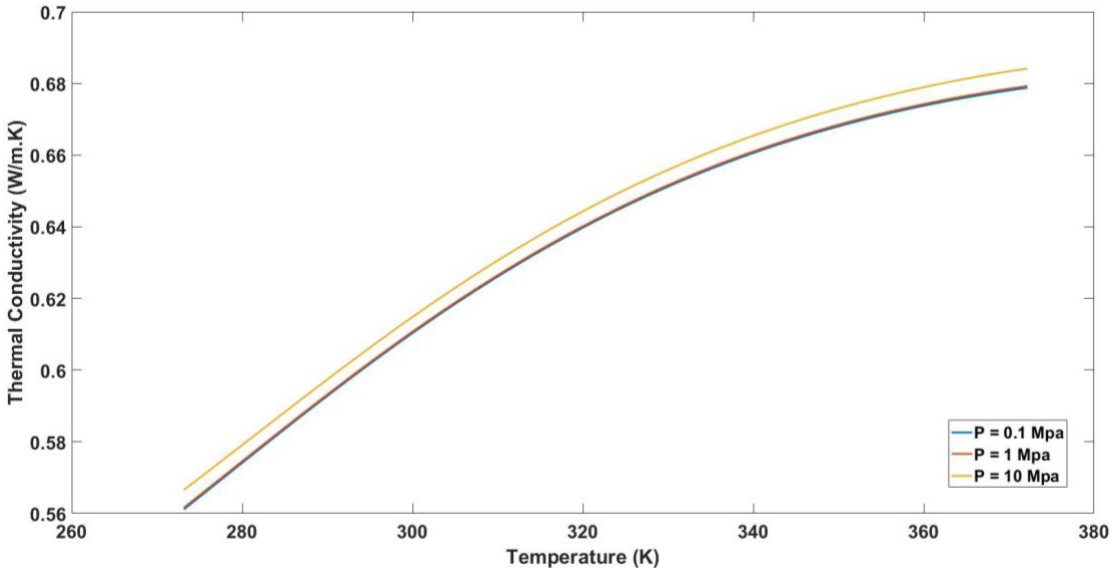

Dynamic viscosity vs Temperature